Winter Weather Forecasting throughout the Eastern United States. Part II: An Operational Perspective of Cyclogenesis

JAMES J. GURKA,* EUGENE P. AUCIELLO,+ ANTHONY F. GIGI,#,## JEFF S. WALDSTREICHER,@,@@ KERMIT K. KEETER,& STEVEN BUSINGER,**,&& AND LAURENCE G. LEE&,†

*NOAA, NWS Forecast Office, Taunton, Massachusetts; +NOAA, NWS Headquarters, Silver Spring, Maryland; #NOAA, NWS Forecast Office, New York, New York; @NOAA, NWS Eastern Region Headquarters, Scientific Services Division, Bohemia, New York; &NOAA, NWS Forecast Office, Raleigh-Durham, North Carolina; **Department of Marine, Earth and Atmospheric Sciences, North Carolina State University, Raleigh, North Carolina

(Manuscript received 16 December 1992, in final form 28 August 1994)

ABSTRACT

The complex combination of synoptic and mesoscale interactions, topographic influences, and large population densities poses a multitude of challenging problems to winter weather forecasters throughout the eastern United States. Over the years, much has been learned about the structure, evolution, and attendant precipitation within winter storms. As a result, numerous operational procedures, forecast applications, and objective techniques have been developed at National Weather Service offices to assess the potential for, and forecast, hazardous winter weather. A companion paper by Maglaras et al. provided an overview of the challenge of forecasting winter weather in the eastern United States.

This paper focuses on the problem of cyclogenesis from an operational perspective. Since pattern recognition is an important tool employed by field forecasters, a review of several conceptual models of cyclogenesis often observed in the east is presented. These include classical Miller type A and B cyclogenesis, zipper lows, 500-mb cutoff lows, and cold-air cyclogenesis. The ability of operational dynamical models to predict East Coast cyclones and, in particular, explosive cyclogenesis is explored. An operational checklist that utilizes information from the Nested Grid Model to forecast the potential for rapid cyclogenesis is also described. A review of signatures related to cyclogenesis in visible, infrared, and water vapor satellite imagery is presented. Finally, a study of water vapor imagery for 16 cases of explosive cyclogenesis between 1988 and 1990 indicates that an acceleration of a dry (dark) surge with speeds exceeding 25 m s^{-1}, toward a baroclinic zone, is an excellent indicator of the imminent onset of rapid deepening.

1. Introduction

East Coast winter storms bring with them a multitude of forecast problems. In addition to substantial snowfalls, weather hazards such as freezing precipitation, flooding rains, high winds, bitterly cold temperatures, coastal flooding (and beach erosion), and even strong convection often confront forecasters in the East during the cold season. This is the second in a series of papers focused on the synoptic and mesoscale features associated with forecasting winter weather in the eastern United States. This paper looks at the phenomenon of East Coast cyclogenesis from the perspective of an operational forecaster.

Many references in the scientific literature describe the processes that contribute to surface cyclogenesis. An overview of the synoptic and mesoscale features associated with East Coast cyclogenesis were presented in a companion paper by Maglaras et al. (1995). Kocin and Uccellini (1990) furnish a detailed review of the processes and atmospheric flow patterns that interact to produce wintertime extratropical cyclones along the eastern seaboard of the United States. Also, they provide a comprehensive evaluation of the surface and upper-air features that accompanied 20 major East Coast winter storms from 1955 to 1985.

This document focuses on cyclogenesis as a forecast problem and highlights some of the conceptual considerations, methodologies, tools, and techniques employed by today's "frontline" forecasters. The authors recognize that some aspects of cyclogenesis are not discussed here. For those who are looking for a more extensive overview of cyclogenetic theory, Uccellini (1990) provides an excellent discussion on the mechanisms and feedbacks involved in rapid extratropical cyclone development.

Synoptic climatology, pattern recognition, and the application of conceptual models are vital components

Current affiliation: NOAA, NWS, Mount Holly, New Jersey.
@@ Current affiliation: NOAA, NWS, Binghamton, New York.
&& Current affiliation: Department of Meteorology, University of Hawaii at Manoa, Honolulu, Hawaii.
† Current affiliation: NOAA, NWS Office, Greer, South Carolina.

Corresponding author address: Jeff S. Waldstreicher, National Weather Service, 32 Dawes Drive, Binghamton Regional Airport, Johnson City, NY 13790.

of operational forecasting. Section 2 of this paper reviews several patterns of evolution typical of winter cyclones in the East. Section 3 addresses the problem of forecasting explosive cyclogenesis. The performance of the National Meteorological Center's (NMC's) operational dynamical models in forecasting surface cyclogenesis and, in particular, rapidly deepening cyclones is examined. A checklist is also described that was developed for forecasters to highlight the features in dynamical model output that have been correlated with rapidly intensifying storms. Section 4 discusses how satellite imagery is used by forecasters in the eastern United States to evaluate and predict cyclogenesis and, in particular, rapidly deepening cyclones. A summary and concluding remarks are provided in section 5.

2. Patterns of cyclogenesis

Efforts by meteorologists to study and document the salient features of East Coast storm development and climatology can be found in the literature as long as a half-century ago. The studies by Austin (1941) and Miller (1946) provided some of the basic groundwork for many current research endeavors. Mather et al. (1964) and Davis et al. (1993) performed climatological studies of extratropical cyclones along the East Coast and defined eight classes of storms that caused damage to the coastline due to the combined action of wind and waves.

Often overlooked in weather forecasting is the importance of a thorough knowledge of the synoptic climatology of an event of interest. This section will describe certain preferred patterns of cyclogenesis that exist along the East Coast. Forecasters should be aware of the variety of storm types and the typical distribution of sensible weather phenomena associated with each type. For example, some storm types are accompanied by a characteristic distribution of liquid, freezing, and frozen precipitation. Once a forecaster determines the general character of precipitation based on a conceptual model of the storm type, he/she can then focus attention on the details such as the size, orientation, and location of transition zones, and the precipitation amounts. In general, by anticipating the essential characteristics of a cyclogenesis event early in its development, a forecast strategy can be devised that focuses on the most likely problems. The features of the storm that pose the greatest hazards to life and property can be emphasized, often at an earlier stage. Similarly, by employing conceptual models based on recognizing a pattern of cyclogenesis, forecasters can dismiss, or at least downplay, events that are unlikely to occur, or the aspects of a storm that will not have a significant impact.

a. "Classical" Miller cyclogenesis

The Miller (1946) classification of East Coast storm types into two basic categories, "A" and "B" (Fig. 1), remains to this day a useful means of cataloging many cyclogenesis events according to surface features. [Note, the Miller storm types A and B are not related to the type A and type B cyclones described by Pettersen and Smebye (1971).]

Type A development most often occurs along a cold front, typically located over the southern United States, or the Gulf of Mexico. This cold front is usually of polar (or in some cases arctic) origin, separating cold, continental polar air from warm, maritime tropical air. The developing cyclone advances in a steady track along this baroclinic zone, typically moving toward the northeast.

Type B storms consist of a complex circulation pattern involving secondary cyclogenesis. As the primary low occludes and dissipates west of the Appalachians, secondary cyclogenesis begins along a warm front that is commonly shared with the primary low. Typically, the warm front extends to the coastal waters where it connects with shallow boundaries that form locally near the coast (e.g., the coastal front). The secondary low and associated fronts separate the shallow wedge of cold air east of the Appalachians, usually a result of cold-air damming (Richwein 1980), from the warmer air over the Atlantic Ocean.

Figure 1a depicts an extreme example of Miller type A cyclogenesis, the "Superstorm of March 1993" (U.S. Department of Commerce 1994a). While the general track and evolution of this storm is characteristic of a type A event, the central sea level pressure of 984 mb at 0000 UTC 13 March while the storm was in the Gulf of Mexico is about 20 mb deeper than a typical type A storm over that location and at that stage of evolution. Figure 1b shows a typical type B event, with coastal secondary cyclogenesis occurring on a coastal front southeast of the dissipating primary low in the Ohio Valley.

Forecast experience at the Raleigh–Durham National Weather Service Forecast Office (Keeter et al. 1989; Keeter et al. 1993; Keeter et al. 1995) has shown that the width of the transition zone of an icy mix of precipitation varies according to Miller cyclone type. Because of the varying thermal advection patterns that occur in response to the secondary cyclogenesis and the dissipation of the primary low, type B events typically have a broad precipitation transition zone compared to type A events. The well-organized single surface low characteristic of type A events are usually associated with well-established thermal advection patterns, yielding a narrower transition zone of mixed precipitation. As a result, changes in precipitation type at a single location are more likely to occur during a type B event, especially near the southern and eastern periphery of the cold-air mass.

Figure 2 shows a climatological model representing the typical characteristics of the transition zone of mixed precipitation associated with the Miller cyclone types. The pattern shown is for North Carolina, an area that often lies near the southern and eastern pe-

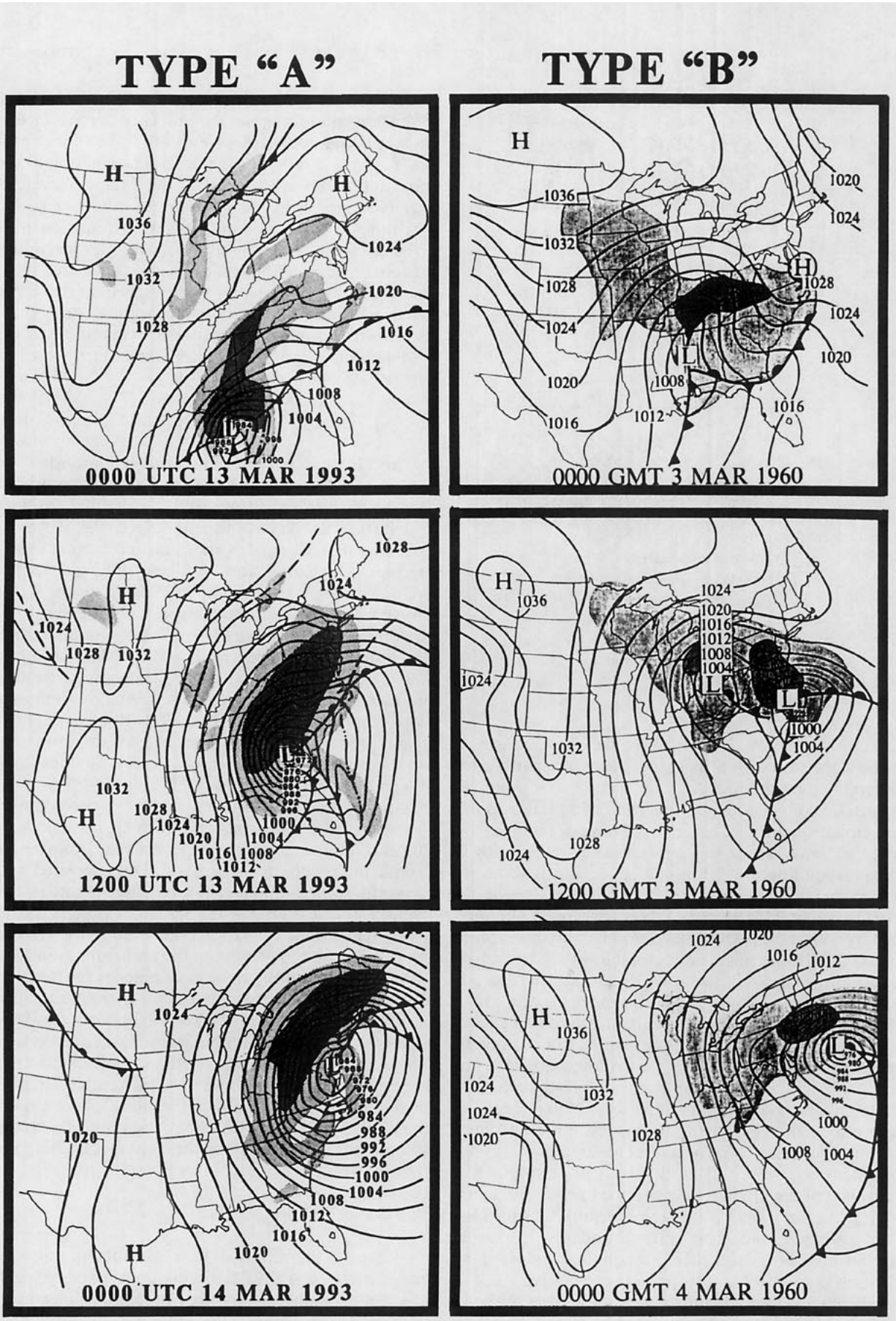

FIG. 1. Examples of Miller type A (left) and Miller type B (right) cyclones [adapted in part from Kocin and Uccellini (1990)].

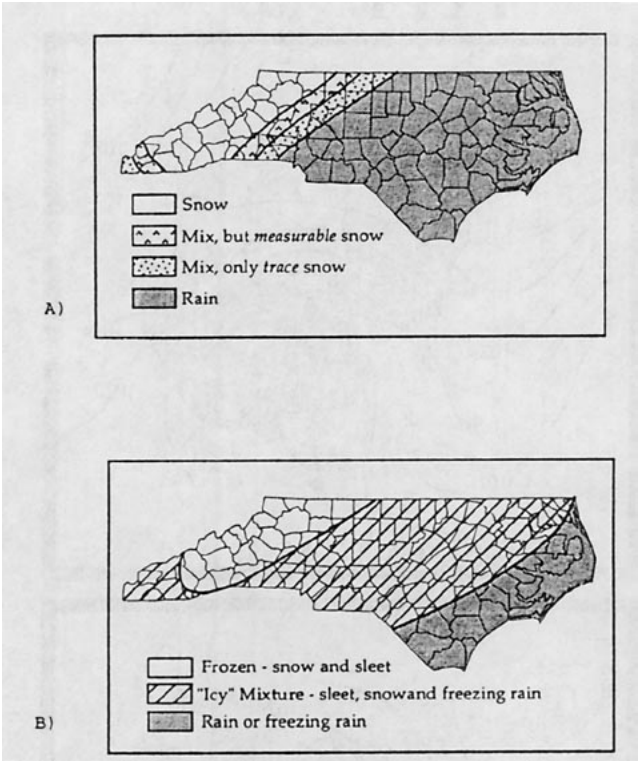

FIG. 2. Conceptual models of precipitation type patterns associated with (a) well-organized Miller type A events and (b) Miller type B and disorganized Miller type A events.

riphery of the cold-air mass. Often the broad transition zone associated with Miller type B events narrows considerably over the mid-Atlantic and New England regions. Of course, much of this narrowing is due to the precipitation moving farther north and deeper into the cold-air mass. However, the transition zone width is also responding to the thermal advection patterns accompanying cyclogenesis. As the inland low dissipates and the coastal low becomes more developed, the variability within the thermal advection pattern diminishes. Accordingly, the migrating coastal low then resembles the more well established and organized thermal advection patterns associated with type A events.

It should also be noted that relatively broad transition zones of mixed precipitation often can occur with weak or disorganized Miller type A lows. Especially in the absence of strong thermal advection, adiabatic and diabatic processes (e.g., melting, evaporative cooling) are often critical in determining precipitation types. Along the East Coast, where cold-air damming is a frequent occurrence, cold, dry air is often in place in advance of the approaching surface low. The diabatic effect of evaporative cooling as moisture falls into the surface-based cold layer often produces a relatively broad area of mixed precipitation. As discussed by Fritsch et al. (1992), this process often feeds back to itself, tending to maintain, or even strengthen, the cold-air mass. This aspect is discussed in greater detail by Keeter et al. (1995).

Beyond using conceptual models of storm types, forecasters must recognize the influence of other factors such as topography upon transition zone characteristics. Figure 2 shows how the general orientation of the transition zones are parallel to the Atlantic coast, in part in response to the moderating influence of the maritime air. Also note the secondary transition zone oriented northwest to southeast over the far southwestern corner of North Carolina. This secondary transition zone with snow to the east and rain, or an icy mix, to the west represents the influence of the mountains limiting the westward penetration of the cold-air dome dammed against the eastern slopes of the Appalachians.

b. "Zipper" lows

The Miller classification scheme is appropriate for the categorization of many East Coast storm events. However, forecasters are well aware that Miller's scheme does not describe the entire spectrum of cyclone evolution. For example, Keshishian and Bosart (1987), expanding on earlier work by Clark (1983), described cyclonic disturbances, termed "zipper lows," that propagate northward along a coastal baroclinic zone. In contrast to the generally more substantial surface development associated with the two Miller (1946) storm types, zipper lows are typically weak features producing little weather of consequence; however, forecasters should recognize the role of the zipper low in modifying the environment to provide a more favorable setting for a subsequent more significant cyclogenesis event.

Zipper lows appear to be related to lower-tropospheric troughs, sometimes not much higher than about 700 mb. Unlike most major East Coast cyclogenesis events, the predominant surface high associated with zipper low development is located offshore rather than over the northeastern United States or eastern Canada. Thus, the surface geostrophic flow along the coast is southerly, which is parallel to the baroclinic zone. The flow in advance of the zipper low pinches the isotherm ribbon together (like a zipper), but there is no significant cold-air advection in its wake. Following the passage of the weak low, a moist baroclinic zone persists. The remaining moisture, surface vorticity, and enhanced baroclinicity can create a favorable environment in the lower levels of the atmosphere for the eventual development and intensification of a second low moving northeast along the coast (Keshishian and Bosart 1987).

c. Late season 500-mb cutoff lows

Adding to the variety of East Coast storm types, Sabones and Keeter (1989) discussed a type of cyclogenesis that occasionally produces late season snow in the western North Carolina mountains. They describe a sharp, deepening trough at 500 mb that eventually

forms a closed low in the vicinity of the southern Appalachians. Cold air near the core of the closed quasi-barotropic low can produce a lower-tropospheric thermal structure that allows snow to penetrate downward to the surface, which is generally above 610 m (2000 ft) MSL across the southern Appalachians. Orographic effects of upslope flow from the associated surface low can help to sustain enough cold air to support snow. The characteristically slow motion of these storms can result in prolonged precipitation and substantial snow accumulations.

An example of this type of event is the slow-moving storm system during 2–5 April 1987, which produced heavy snow across much of the southern Appalachian region, with accumulations of 100–150 cm (40–60 in.) at several locations in the North Carolina mountains. Similarly, on 12 April 1988, cold air associated with a closed low moved into North Carolina *from the south,* contributing to snowfall that reached 46 cm (18 in.).

A familiarity with the cutoff low cyclogenesis pattern can help the forecaster anticipate the unlikely (from a climatological perspective) event of a late season heavy snow. Fishel and Businger (1993) describe an event that occurred 6–8 May 1992 when a nearly stationary 500-mb closed low (Fig. 3) dropped 75 cm (30 in.) of snow on the weather station on Mount Mitchell (elevation 1890 m or 6240 ft), with unofficial accumulations reported as high as 150 cm (60 in.) atop Mount Pisgah (elevation 1733 m or 5721 ft). Measurable snow (0.5 cm or 0.2 in.) was recorded at the National Climatic Data Center's weather station in downtown Asheville, North Carolina, for the first time in May since official records began in 1902 (U.S. Department of Commerce 1992a).

While cutoff 500-mb lows present forecasters in the Carolinas with the threat of late season heavy snows, they are a considerable forecast problem throughout the eastern United States. On 10–14 December 1992, an upper trough closed off in the vicinity of the Chesapeake Bay. The system became vertically stacked, and remained nearly stationary along the mid-Atlantic coast (Fig. 4). With a strong surface high anchored over the Canadian maritimes, strong onshore winds {Ambrose Tower just outside New York Harbor recorded hurricane force winds [sustained 36.2 m s^{-1} (70 kt)] with gusts to 41.6 m s^{-1} (81 kt)} battered the coastline from southern New England to New Jersey for several tidal cycles, producing major coastal flooding and widespread severe beach erosion (National Weather Service 1994). Several major thoroughfares in the New York City area were inundated. In addition, the slow movement of the storm produced widespread snowfall of 30–60 cm (1–2 ft) across inland areas from Massachusetts, Connecticut, and Rhode Island to western New York and the mountains of western Pennsylvania, western Maryland, and the panhandle of West Virginia. The greatest snow accumulations were in the Berkshires of western Mas-

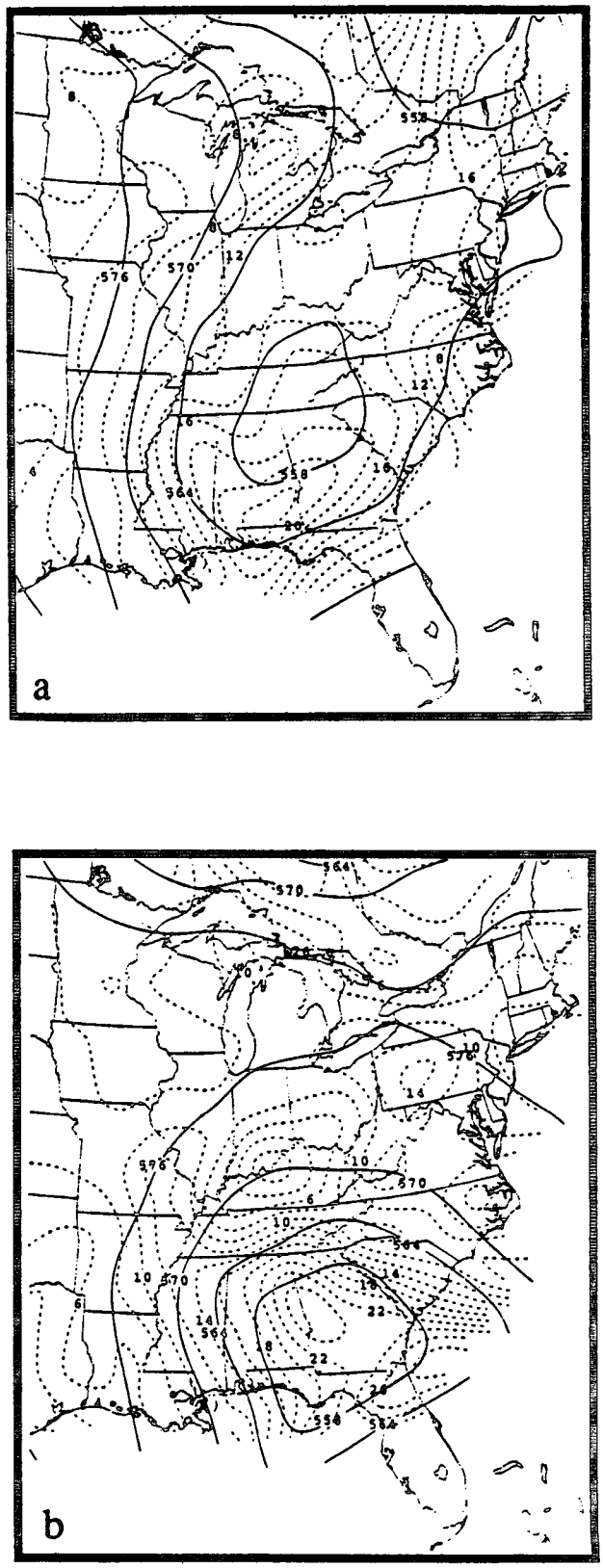

FIG. 3. Analysis of 500-mb heights (dm; solid lines) and absolute vorticity ($\times 10^{-5}$ s^{-1}; dashed lines) for (a) 0000 UTC 7 May 1993 and (b) 0000 UTC 8 May 1992.

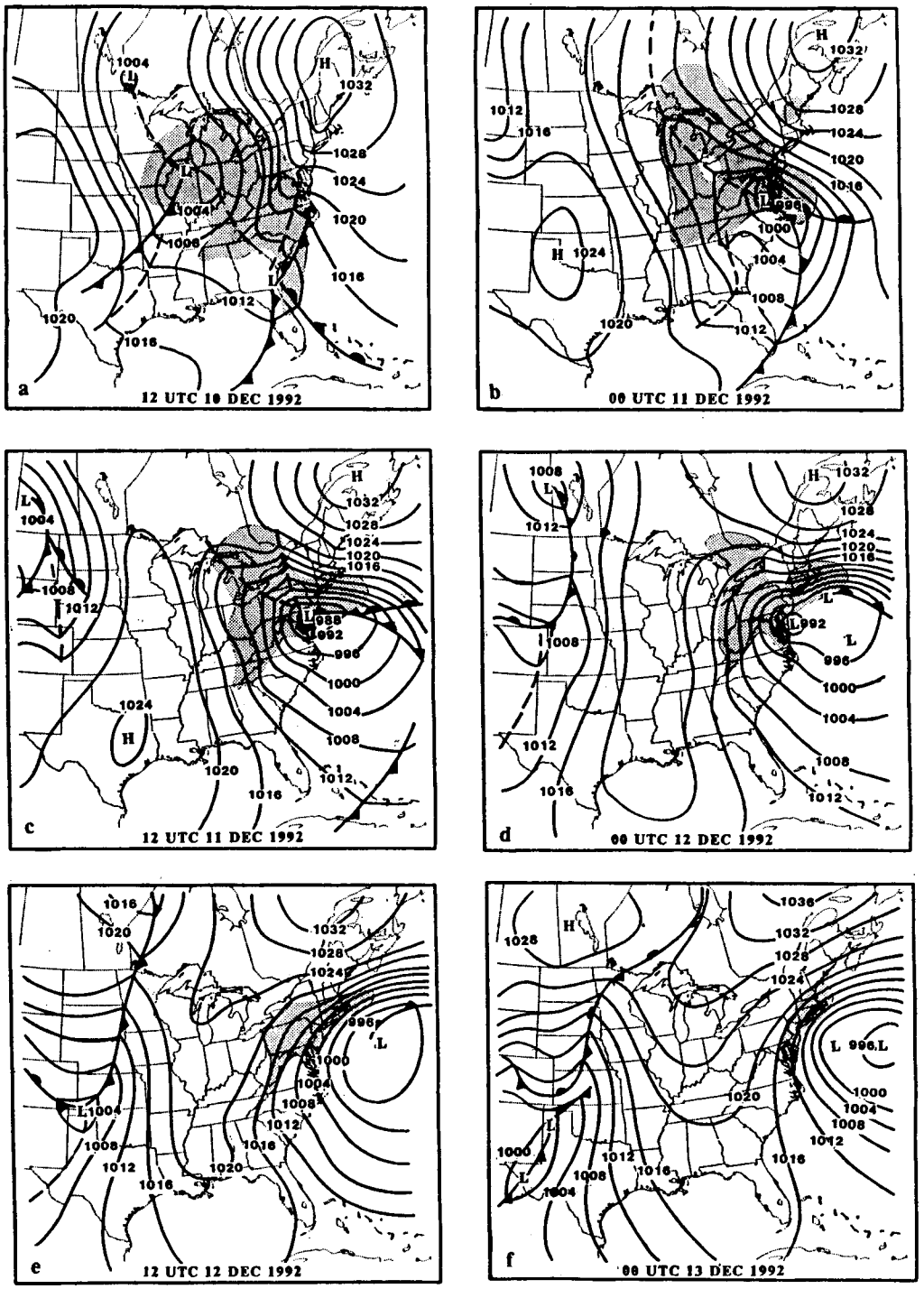

FIG. 4. Sea level pressure analysis for (a) 1200 UTC 10 December 1992, (b) 0000 11 December 1992, (c) 1200 UTC 11 December 1992, (d) 0000 12 December 1992, (e) 1200 UTC 12 December 1992, and (f) 0000 13 December 1992. (Adapted from National Weather Service 1994.)

sachusetts, the Catskills of southeastern New York, and Garrett County in extreme western Maryland, where up to 90–120 cm (3–4 ft) fell (National Weather Service 1994).

d. Cold-air cyclogenesis

A fourth type of East Coast cyclogenesis occurred on 24 February 1989 when a small synoptic-scale cy-

clone formed along the mid-Atlantic coast of the United States during a cold-air outbreak. The storm brought high winds and moderate to heavy snow to the mid-Atlantic coast (Fig. 5). This event is especially noteworthy because development occurred in the cold air following a surface cold front that crossed the East Coast on 22 February. Although cold-air cyclogenesis (relative to the 1000–500-mb thickness ribbon) has been the subject of active research in recent years (e.g., Businger and Reed 1989), few cases along the eastern seaboard of the United States have been investigated with the advantage of in situ data. [See Bosart and Sanders (1991) for another example of cyclogenesis that occurred on the cold side of the baroclinic zone.] The three-dimensional structure of this cold-air cyclone is examined through analysis of NOAA P-3 aircraft data, drifting buoy, operational National Weather Service data, and satellite imagery available for Intensive Observing Period (IOP) No. 8 of the Experiment on Rapidly Intensifying Cyclones over the Atlantic (ERICA; Hadlock and Kreitzberg 1988).

Prior to cyclogenesis on 24 February 1989, a shallow east–west-oriented baroclinic zone formed through a combination of shear deformation and differential diabatic heating. The baroclinic zone extended from an offshore frontal wave to eastern North Carolina, and displayed warm frontal characteristics. Satellite imagery and surface streamline analysis revealed a series of vortices (A, B, and C) along this shallow baroclinic zone in a region of enhanced sensible heat fluxes (Fig. 6).

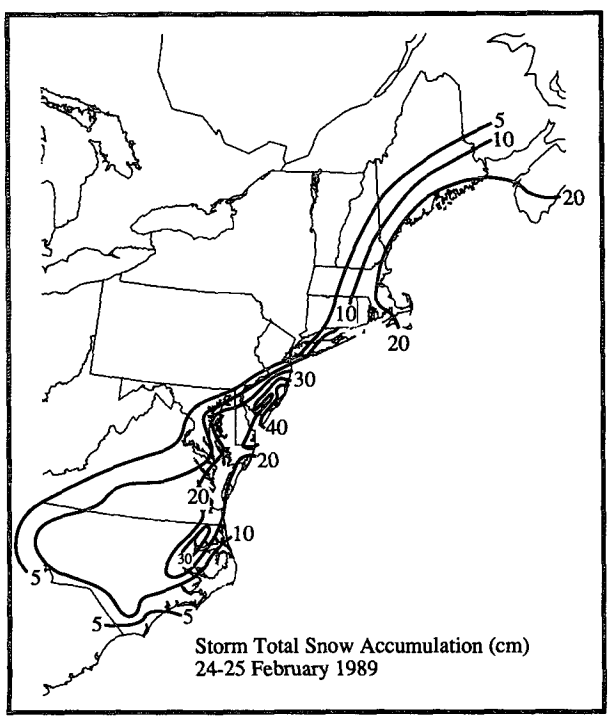

FIG. 5. New snow accumulation (cm) from 1200 UTC 23 February to 1200 UTC 26 February 1989.

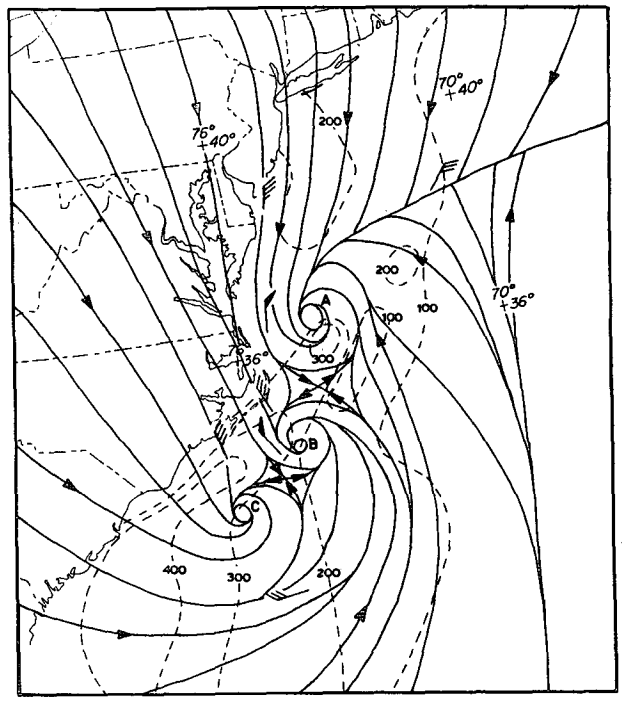

FIG. 6. Surface streamline analysis (solid lines) for 1500 UTC 24 February 1989 (based in part on cloud-street analysis from visible satellite imagery), and sensible heat flux (W m^{-2}; dashed lines) for 1200 UTC 24 February 1989.

Baroclinic forcing associated with a pronounced upper-level short wave (Fig. 7) triggered rapid surface cyclogenesis in low-level vortex A (Fig. 8). The most rapid deepening (sea level pressure drop of 12 mb in 12 h) occurred during the initial stage of development, coincident with the development of a narrow band of deep convection oriented parallel to the mid-Atlantic coast of the United States. The band of convection was associated with a region of pronounced cyclonic vorticity advection aloft, and was embedded in a broader region of stratiform precipitation. The low subsequently tracked northeastward, maintaining its strength, reaching Nova Scotia on 26 February.

This event produced a particular forecast challenge because of the large snowfall gradient (Fig. 5) along the highly populated Interstate 95 corridor that runs, in part, from New York City, to Philadelphia, to Washington, D.C. The snowfall gradient was particularly enhanced across New Jersey. Atlantic City, New Jersey, received approximately 48 cm (19 in.) of snow, while much the New York City metropolitan area received only trace amounts. This event was termed by Gigi (1989) as "the New York City snowstorm that never was."

3. Forecasting explosive cyclogenesis

In addition to recognizing the various patterns of cyclogenesis, East Coast forecasters must anticipate and

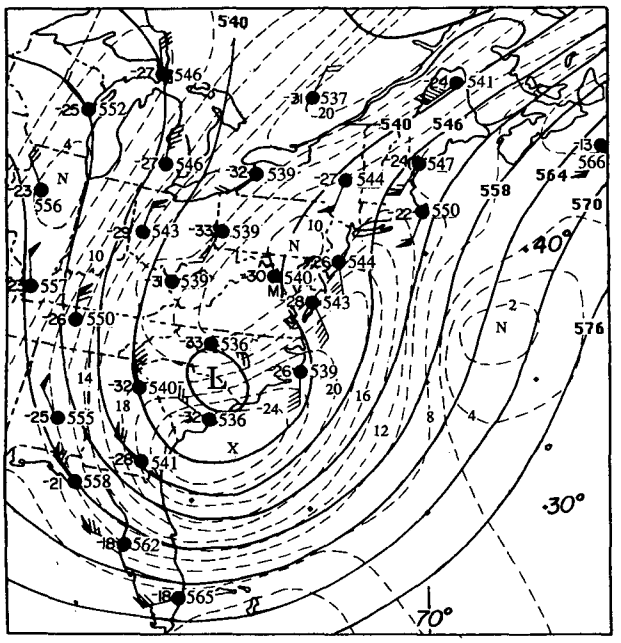

FIG. 7. Analysis of 500-mb heights (dm; solid lines), and absolute vorticity ($\times 10^{-5}$ s^{-1}; dashed lines) for 1200 UTC 24 February 1989. Station plots include heights (dm), temperatures (°C), and winds [pennants = 25 m s^{-1}, full (half) barb = 5 (2.5) m s^{-1}].

evaluate the potential for explosive cyclogenesis. In the Atlantic, the most prominent region of high-frequency explosive cyclogenesis extends from the coastline of the Carolinas, northeast across Georges Bank to south of Newfoundland (Roebber 1984). Explosive maritime cyclones, often referred to as meteorological bombs, are a significant winter weather concern to operational meteorologists in the eastern United States. Of primary importance to marine forecasters is the threat of storm force winds (greater than 24 m s^{-1} or 47 kt) associated with these bombs. Public forecasters are most concerned with the potential for heavy snowfall, and the storm surge associated with these storms that can result in substantial coastal flooding and erosion.

A meteorological bomb was arbitrarily defined by Sanders and Gyakum (1980) as an extratropical surface cyclone whose central pressure dropped an average of at least 1 mb h^{-1} for 24 h at 60°N, normalized geostrophically at other latitudes. Sanders (1986) studied explosive cyclogenesis in the west central North Atlantic Ocean. A high correlation was found between upper-level cyclonic vorticity advection over the surface cyclone and simultaneous surface deepening rate. Thus, the explosive maritime cyclone is fundamentally a baroclinic disturbance in which the low-level response to upper-level forcing is dramatically large.

a. Dynamical model forecast performance

Studies by Leary (1971) and Silberberg and Bosart (1982) were among the initial efforts to assess the performance of the National Meteorological Center (NMC) dynamical models in forecasting surface cyclones. More recently, Junker et al. (1989), Grumm and Siebers (1989), and Grumm et al. (1992) examined overall systematic cyclone forecast errors of NMC's regional models, particularly the Nested Grid Model (NGM; Hoke et al. 1989). Similarly, Grumm and Siebers (1990) and Grumm (1993) determined the characteristics of cyclone forecasts from the aviation run (AVN) of NMC's global spectral model, while Smith and Mullen (1993) conducted a comparative study of NGM and AVN forecasts. [The AVN is the spectral model component (Sela 1980) of the NMC Global Data Assimilation and Forecast System (Kanamitsu 1989)].

All of the studies showed the dynamical model forecasts of surface cyclones were skillful, although several important systematic errors were noted. Grumm et al. (1992) state that, in general, NGM surface cyclones tended to be too deep (primarily due to the model being too slow to increase the central pressure of filling cyclones) and move too slowly. However, Grumm et al. (1992) also noted that the NGM was too slow to reduce the surface pressure of deepening cyclones, and was too slow to develop surface cyclones over warm waters, especially near the Gulf Stream. Smith and Mullen (1993) found similar results. In contrast, Grumm and Siebers (1990), Grumm (1993), and Smith and Mullen (1993) found that, overall, the central pressure of AVN surface cyclones was not deep enough. All three studies found that the AVN generally outperformed the NGM in forecasting the placement and central pressures of surface cyclones.

One particularly interesting result of the Smith and Mullen (1993) study was that an equally weighted average of the NGM and AVN output produced a superior forecast, on average, than either individual model. This improvement increased as the differences between the specific NGM and AVN forecasts increased. This tendency for a superior "compromise" solution, particularly when the model solutions diverge, is an approach many field forecasters have employed intuitively for some time. Recently, NMC has moved toward more direct applications of this approach by implementing an operational ensemble prediction scheme (Tracton and Kalnay 1993).

Sanders (1987b) specifically addressed cases of explosive cyclogenesis by examining the predictive skill of the NGM (out to 48 h) and the Global Spectral Model (out to 60 h). Sanders found that both models displayed skill in forecasting rapidly deepening cyclones. Oravec and Grumm (1993) studied the performance of the NGM in predicting rapidly deepening cyclones for a 3-year period from the winter of 1988–89 to the autumn of 1991. They also found that the NGM had considerable skill, although the model's ability to forecast rapidly deepening storms decreased steadily with forecast length through 48 h. The ability of the NGM to detect rapidly deepening cyclones was

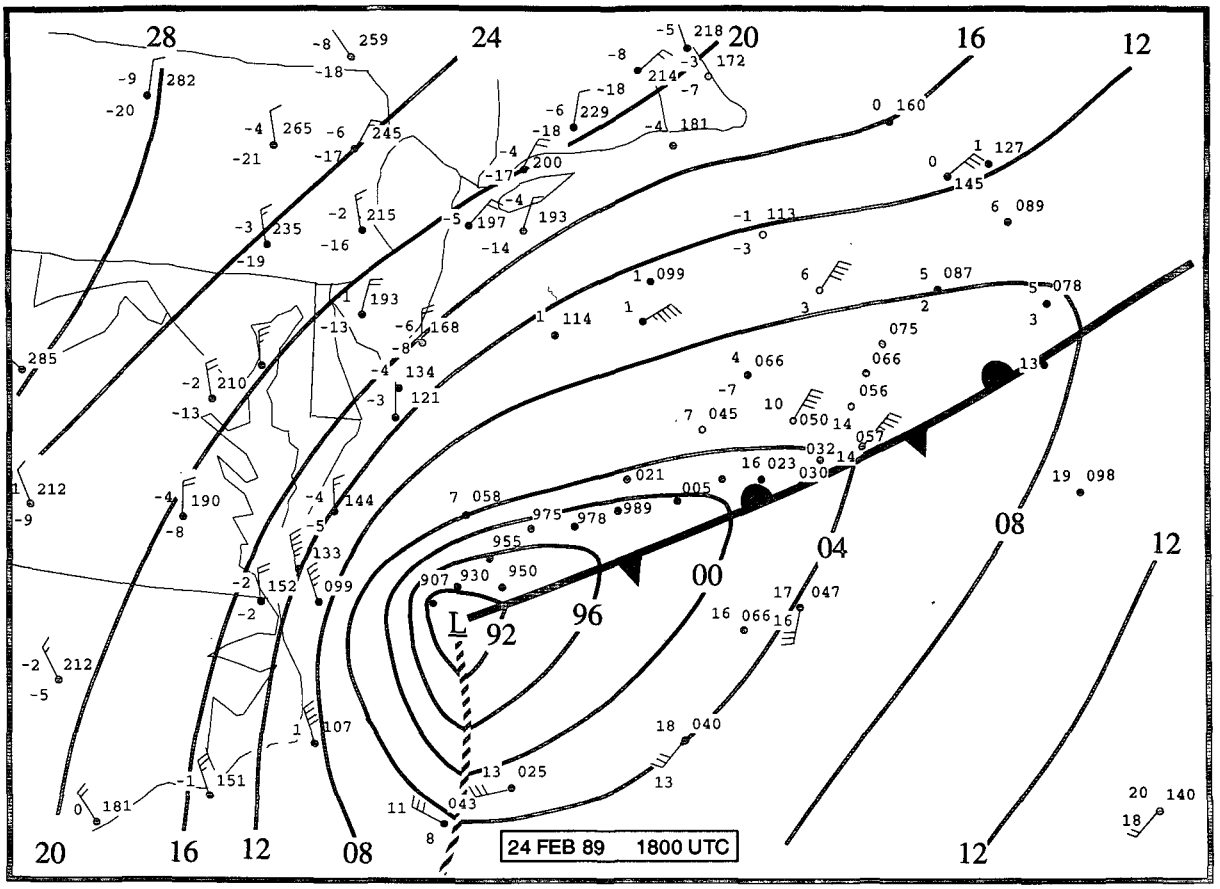

FIG. 8. Surface pressure analysis (mb) for 1800 UTC 24 February 1989.

greatest in winter, with skill decreasing in the spring and fall.

Oravec and Grumm (1993) also noted several characteristics of NGM simulations of rapidly deepening cyclones. These results indicated the NGM was too slow to deepen rapidly deepening cyclones, and too slow to move such storms to the east, although the overall position errors were less than the position errors for all NGM cyclones. However, the NGM did not show exceptional skill in correctly forecasting the 12-h pressure trends of rapidly deepening cyclones.

Sanders (1992) examined the performance of the Medium Range Forecast (MRF) runs from NMC's Global Spectral Model (Kanamitsu 1989) during the ERICA project. The MRF displayed skill in the prediction of 500-mb planetary- and smaller-scale waves out to ranges of 5 days. The model also showed skill in forecasting the location and deepening rate of surface cyclones within the ERICA region (Hadlock and Kreitzberg 1988) out to 5 days. Finally, the MRF also showed the ability to distinguish explosively deepening cyclones from others at all ranges, although the skill decreased to small values by day 5.

Sanders and Auciello (1989) compared analyses and predictions of explosive cyclogenesis over the western North Atlantic Ocean. The analyses included the manual and automated series produced at NMC. The forecasts were those produced by the NGM and the aviation run of the Global Spectral Model at NMC, and also by a checklist developed by Auciello and Sanders (1986, 1987). This operational checklist has been utilized by meteorologists at several East Coast Weather Service Forecast Offices (WSFO) for the past several cold seasons. Sanders and Auciello (1989) found that there has been a considerable increase in skill of operational dynamical models at NMC in the prediction of explosive cyclogenesis, and that the accuracy of the checklist forecasts was comparable. The checklist's primary value, however, was in alerting forecasters to the potential of explosive cyclogenesis, and the typical predecessor conditions.

b. The bomb checklist

The explosive cyclogenesis checklist was developed by Auciello and Sanders (1986 and 1987) from the results of a 1985 workshop on oceanic storms reported by Lange et al. (1986). The checklist was designed as an objective operational technique for the prediction of meteorological bombs and resultant storm force

winds up to 36 h prior to the event. Tracks and central values of surface low pressure centers and 500-mb absolute vorticity maxima were investigated for 48 cases of explosive cyclogenesis that occurred between January 1981 and November 1984 over an area between 38° and 45°N and 55° to 75°W. These cases were stratified into strong, moderate, and weak intensity categories. Weak bombs were omitted from the analysis since such events do not normally produce storm force winds. The mean evolutional characteristics of the remaining 28 strong and moderate bombs was the basis of the explosive cyclogenesis checklist.

The checklist, as used with the NGM analyses and forecasts, comprises six categorical questions (Table 1). Explosive cyclogenesis is predicted when four or more of the questions are answered affirmatively. This checklist criterion was selected subjectively through an examination of explosive cyclogenesis events during preceding seasons. No study has been made to determine if the criterion is optimal or to what extent the questions may be redundant. Assuming a perfect prognosis of NGM-produced 500-mb vorticity, time zero (the midpoint of the 24-h period of maximum deepening) will occur when the overtaking 500-mb vorticity maximum is, on the average, 250 nm west of the surface low. Operational experience has shown that the onset of storm force winds occurs close to time zero.

The first four checklist questions deal exclusively with NGM-produced 500-mb absolute vorticity maxima. A vorticity maximum of at least 17×10^{-5} s^{-1} must exist as an initial NGM condition in a spawning area between 30° and 50°N and 85° to 110°W. Movement must average at least 15.5 m s^{-1} (30 kt). This speed of movement provides the strong dynamical impetus necessary for explosive development. Vorticity maxima must cross the coast between 32° and 45°N, indirectly incorporating the strong sea surface temperature gradient along the north wall of the Gulf Stream into the evaluation.

These values were based on the preliminary results of Sanders (1987a) examination of the intensity, speed, and latitudinal crossing of 500-mb absolute vorticity maxima and associated cyclogenesis in the western North Atlantic during the 1986–87 cold season. Investigations showed that 40% of the upper-level vorticity maxima crossing the east coast of North America (between 20° and 60°N lat) during this time period produced meteorological bombs. However, 53% of the vorticity maxima crossing south of 41°N produced bombs, while only 26% of the cases crossing north of this latitude resulted in rapidly deepening surface cyclones. Similarly, Sanders found that 47% of the vorticity maxima that tracked at speeds greater than 15.5 m s^{-1} (30 kt) resulted in bombs, while those traveling slower produced bombs only 26% of the time. Finally, it was found that the best discriminator was when the speed of the vorticity maximum was multiplied by the vorticity intensity, which is an indicator of the strength of the 500-mb vorticity advection (e.g., the degree of baroclinic forcing).

TABLE 1. The explosive cyclogenesis checklist for the North Atlantic Ocean.

1) Does a 500-mb absolute vorticity maximum of 17×10^{-5} s^{-1} or greater exist in the NGM initial analysis over an area between 30° to 50°N and 85° to 110°W?
2) Does this 500-mb vorticity maximum maintain initial intensity or strengthen on successive 12-, 24-, 36-, and 48-h NGM charts?
3) Is this 500-mb vorticity maximum forecast to move an average of 30 kt or greater through 48 h?
4) Does the initial NGM-produced 500-mb vorticity maximum cross the coast between 32° and 45°N?
5) Does a jet streak of 110 kt or greater exist at 250 or 300 mb within a 300-nm radius in the semicircle south of the initial 500-mb vorticity maximum?
6) Does the NGM develop a surface low of 990 mb or deeper during the next 48 h over an area between 38° to 45°N and 55° to 75°W?

The inclusion of jet streaks in question 5 serves to reinforce the existence of strong baroclinicity. During the 1985 oceanic storms workshop (Lange et al. 1986), it was noted that, in the early stages of explosive development, an upper-level jet streak is usually present within a 300-nm radius for the semicircle south of the initial 500-mb vorticity maximum. Experience and refinement of the checklist has resulted in the establishment of the 110-kt (55 m s^{-1}) threshold.

The final checklist question refers to the existence of an NGM-produced surface low of 990 mb or deeper over the forecast area between 38° and 45°N and 55° to 75°W. The NGM usually develops a new surface low in the western North Atlantic in response to upper-level forcing. According to Sanders (1986), the vorticity maximum responsible for rapid deepening normally preexists the surface low. The motion of the vorticity maximum relative to the surface low is a counterclockwise spiral beginning to the northwest of the nascent bomb and ending to the south of the developed storm. Strong bombs are differentiated from moderate bombs by the substantially greater initial separation distance and the greater relative speed of the vorticity maximum.

Completed checklists were compiled at WSFO Boston for each run of the NGM during the cold season, 1 October through 31 March, for the 1987–88, 1988–89, and 1989–90 seasons. Individual cases were examined when four or more questions were answered affirmatively. These were denoted forecast episodes. Consecutive checklists referring to the same cyclone were treated as a single episode. A particular cyclone, whether it qualified as a bomb during a single 24-h period, or for overlapping periods, was considered a single event. To be classified as an event (E), a cyclone had to qualify as a bomb within the area between 38° and 45°N and 55° to 75°W. A hit (H) was scored when a cyclone qualified as a bomb in the forecast area at some time from zero to 36 h after a forecast episode.

If no bomb occurred in the area within the time range for any of the checklists in an episode, that forecast was denoted a false alarm (FA). If a bomb occurred and was not within the time range for any checklist with four or more affirmative answers, the event was denoted a miss. The probability of detection (POD = H/E), false alarm ratio (FAR = FA/(FA + H), and critical success index (CSI = $[(POD)^{-1} + (1 - FAR)^{-1} - 1])^{-1}$ were calculated for each cool season.

From 1 October 1987 through 31 March 1988, 15 events were observed within the verification area. The explosive cyclogenesis checklist forecast 18 episodes accounting for 12 hits and 6 false alarms. These data resulted in a POD of 0.80, FAR of 0.33, and CSI of 0.57, respectively.

Sixteen meteorological bombs were observed within the verification area during the 1988–89 season. The checklist scored 13 hits and produced seven false alarms yielding POD, FAR, and CSI of 0.81, 0.35, and 0.57, respectively, close to the values for the 1987–88 season.

During the 1989–90 season, there were 13 explosive cyclogenetic events within the checklist verification area, of which eight were hits. There were 18 false alarms. The POD was thus 0.62, the FAR was 0.69, and the CSI was 0.26. This represents a considerable decline in performance compared to the preceding seasons. No verification of the specific NGM forecasts was undertaken to determine the cause of the poorer checklist performance. Also, no effort has been made to examine the checklist performance during subsequent seasons.

False alarm recognition and common pitfalls in checklist completion were reviewed for earlier seasons (Auciello 1989; Auciello and Sanders 1988). In almost all cases, potential false alarms could be recognized by the absence of a deep, surface low forecast by the model over, or near the forecast area (question 6 in Table 1).

4. Satellite techniques

The explosive cyclogenesis checklist can successfully predict the majority of East Coast bombs. However, with any forecast technique, there will be misses and false alarms. Therefore, it is important for forecasters to recognize situations when rapid cyclogenesis is occurring or imminent, especially if it is not forecast by the models. Satellite imagery, when used in conjunction with other data sources (e.g., surface and upper-air data, dynamical model output, etc.), can aid in the detection and forecast of rapid cyclogenesis. This section discusses how satellite imagery features and interpretation techniques can enhance the forecaster's four-dimensional picture of cyclogenesis events, and aid in evaluating dynamical model forecasts of these events.

Two factors that play a role in explosive cyclogenesis are convection and an upper-level trigger. It has been suggested (by Traction 1973; Bosart 1981; Gyakum 1983) that convective cells near the storm center play an active role in contributing to and even initiating rapid cyclogenesis, primarily through latent heat release. However, the precise role convection plays in the cyclogenesis process is still not clear, and is the subject of continuing research (Uccellini 1990). Convection is generally easily recognizable on visible and window channel infrared (IR) imagery, and in many cases on the moisture channel IR.

Regarding upper-level triggers, Weldon (1979) discusses cloud patterns on visible and IR satellite imagery associated with upper troughs, ridges, vorticity maxima, and jet stream axes. Furthermore, Weldon (1975) described cloud patterns associated with the evolution of winter storms, while Weldon (1985) and Weldon and Holmes (1991) discuss patterns in the moisture channel imagery associated with cyclogenesis. The following is a summary of some of the satellite observable features associated with cyclogenesis.

a. Visible and window channel IR imagery

Features on visible and window channel IR imagery associated with cyclogenesis include the following: (a) an increase in the width of the cloud band associated with the warm front (Anderson 1987); (b) an increase in vertical thickness of the clouds, indicated by cloud top cooling (Anderson 1987; Scofield 1990); (c) the appearance of anticyclonic curvature on the cold-air side of the main cloud band (Anderson 1987); (d) the appearance of mesoscale streaks of upper and mid clouds along the anticyclonically curved boundary of the cloud mass (Anderson 1987); (e) initiation of wave formation as a comma cloud approaches a frontal band (Anderson 1987); (f) the poleward edge of the cloud mass becoming sharper and better defined with time (Weldon 1975); (g) the evolution of a comma pattern possibly from a "leaf" or subsynoptic-scale system (Weldon 1975; Smigielski and Ellrod 1985; Scofield 1990); (h) a rapid increase in convection or sometimes just a persistence of convection (Scofield 1990); and (i) explosive or rapid deepening often occurs when a baroclinic zone cloud band shows a bulging or convex appearance that is increasing rapidly with time (Smigielski and Ellrod 1985).

Using many of these signatures, efforts have been made to categorize extratropical cyclogenesis events based on their evolution as depicted by satellite imagery. Browning and Hill's (1985) three types of cyclogenesis [described in detail in Browning (1990)]: comma development; "instant" occlusion; and frontal wave sequence were found in a review by Evans et al. (1994) to encompass most other proposed classification schemes. One exception is the "split-flow cyclogenesis" category included in the comprehensive scheme for cyclogenesis over the eastern Atlantic proposed by Young (1993).

In a recent study, Evans et al. (1994) examined visible and infrared satellite imagery from 50 explosive cyclogenesis events during the 1970s and 1980s, 46 of which occurred over the western North Atlantic. They

TABLE 2. Summary of the Evans satellite classification scheme of cyclogenesis (from Evans et al. 1994).

Characteristics	Emerging cloud head	Comma cloud	Left exit	Instant occlusion
Satellite imagery	Cloud head emerges poleward of polar-front cloud band	Comma cloud develops independently of polar-front cloud band	Baroclinic leaf rotates as it merges with polar-front cloud band	Cloud cluster is carried downstream to polar-front cloud band
Surface	Development along polar front	Development upstream of polar front	Development slightly upstream of polar front	Development upstream of polar front
Upper-level flow shape	Small-amplitude, initially confluent trough	Increasingly diffluent trough	Large-amplitude, increasingly diffluent trough	Large-amplitude, confluent trough
Relationship of jet streak to surface deepening	Left-exit deepening	Left-exit deepening	Left-exit deepening	Entrance-region deepening

developed a satellite-based classification scheme differentiating between various types of rapid deepening maritime cyclogenesis events. The four types are summarized in Table 2 and shown in Fig. 9.

Common ground can be found between the Evans scheme and many of the nonsatellite-based techniques discussed in section 2. For example, the "emerging cloud head" appears to be very similar to Miller (1946) type A development described in section 2a, while the "left exit" and "instant occlusion" categories has several features common to Miller type B cyclogenesis. Similarly, the development upstream of the polar front depicted in the "comma cloud" and "instant occlusion" cyclogenesis categories is common to the cold-air cyclogenesis events described in section 2d.

To provide a more direct link between the top down observation of satellite imagery and conventional surface pressure analysis, Junker and Haller (1980) devised a satellite-based technique for estimating the central surface pressure of oceanic cyclones that utilized many of the features described by Evans among others. An examination of satellite data and associated ground truth from ERICA (Hadlock and Kreitzberg 1988; Anderson 1989) provided the impetus to update the Junker–Haller technique. The result was the Smigielski–Mogil–Burtt (SMB) technique (Smigielski and Mogil 1991, 1992).

The SMB technique was developed by utilizing the Dvorak (1984) technique of estimating maximum winds and central pressures of tropical cyclones as a

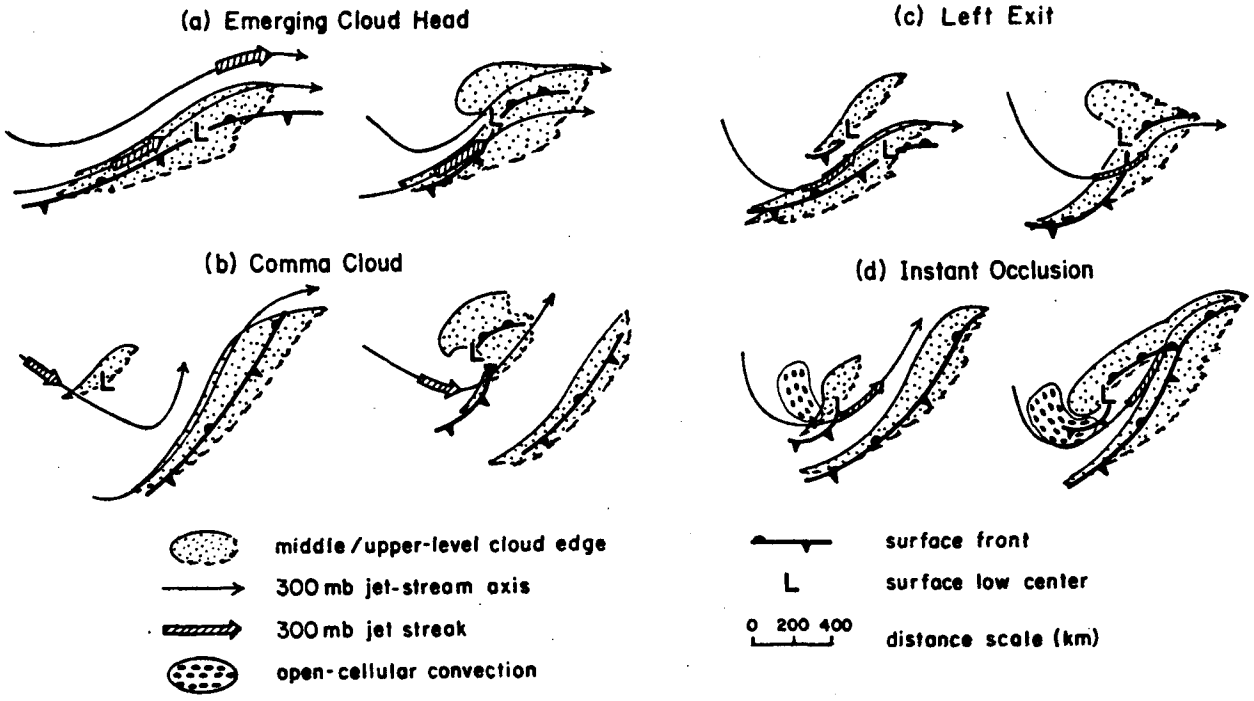

FIG. 9. Schematic representation of the four types of cyclogenesis that compose the Evans satellite classification scheme. Temporal separation between the early (left) and later (right) stages of evolution is approximately 12–24 h (from Evans et al. 1994).

model, and applying it to the extratropical patterns described by Junker and Haller (1980). A conceptual model of storm evolution, in 12-h increments, was devised based on cloud pattern–central pressure relationships for cold season (baroclinic), midlatitude oceanic cyclones, north of 35°N. (Note, only storms over the north Atlantic Ocean were used in the developmental sample.) The result was a systematic pattern recognition flow chart for estimating the minimum central pressures of these ocean storms (Fig. 10). More detailed information on the development and application of the SMB technique can be found in Smigielski and Mogil (1992).

b. The 6.7-μm moisture channel imagery

Examining moisture channel imagery (and other types of satellite data) with conceptual models in mind such as those presented here is helpful in evaluating dynamical model forecasts. For example, the higher temporal and spatial resolution of satellite imagery may better depict important small-scale features that escape or are not sufficiently resolved by observational networks (e.g., radiosondes). If these features are not adequately initialized by a model, its subsequent forecasts will undoubtably suffer. Also, satellite imagery enables the forecaster to track the behavior of features between the current 12-hourly cycle of upper-air observation and model simulations. Gurka (1987) presented five cases where water vapor imagery provided added information beyond the model guidance. (The model forecasts were inadequate for at least three of these events.) This is not to imply that satellite imagery is better than radiosonde data or dynamical model forecasts. Rather, it is meant to highlight the value of satellite information to complement other data sources.

Patterns apparent in the moisture channel imagery associated with cyclogenesis include the following:

(a) Cyclonic surge warming is defined as a warm (dark) zone on the moisture channel imagery, turning into the cyclonic flow, often taking on an elongated shape as it moves into, or becomes, the dry slot southeast of the low. According to Weldon (1985), cyclonic surge warming is often associated with upper-level cyclogenesis, and almost as often with surface deepening. The storm continues to deepen until the surface low moves to the left of the jet, under the core of the upper-cyclonic flow. Examples of cyclonic surge warming have been shown by Gurka (1987) and Funk (1986).

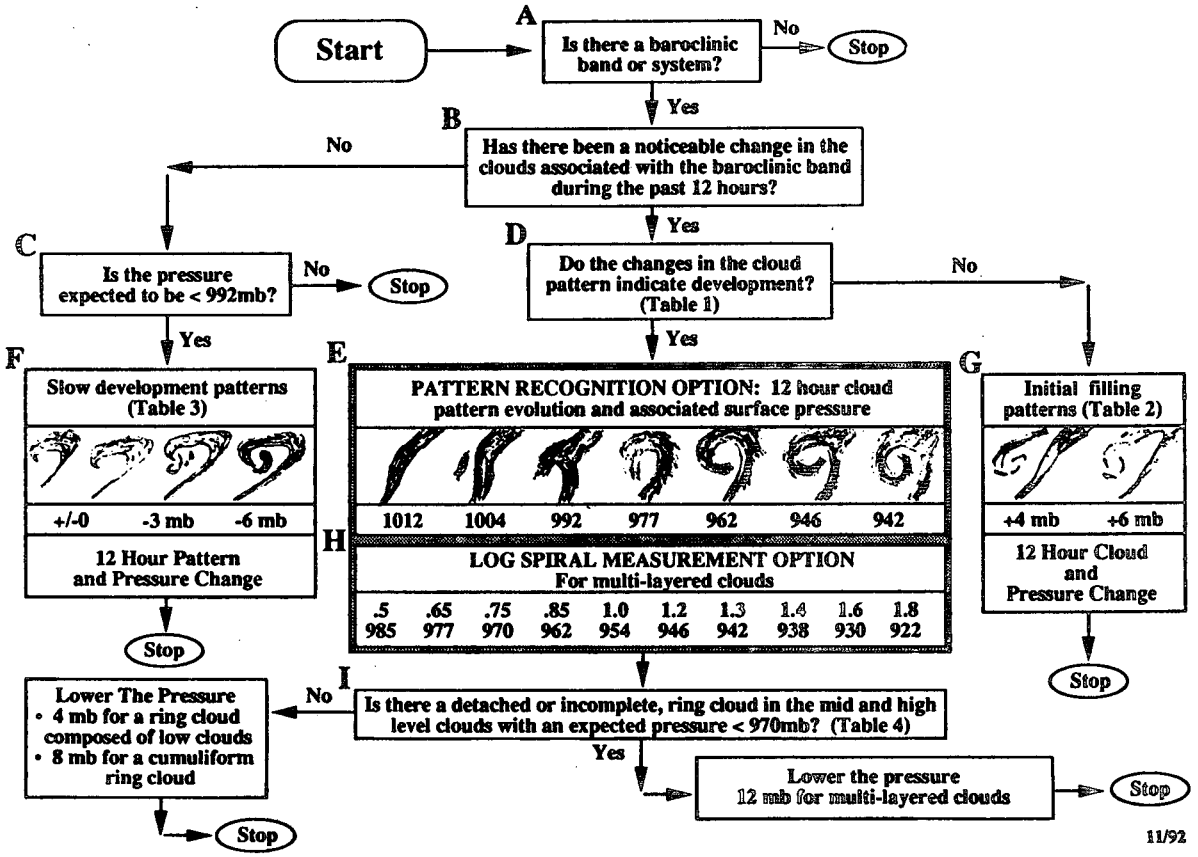

FIG. 10. Flow chart for estimating central pressures of midlatitude North Atlantic Ocean cyclones from satellite cloud patterns and their changes (from Smigielski and Mogil 1992). Tables referred to in the figure are described in Smigielski and Mogil (1992).

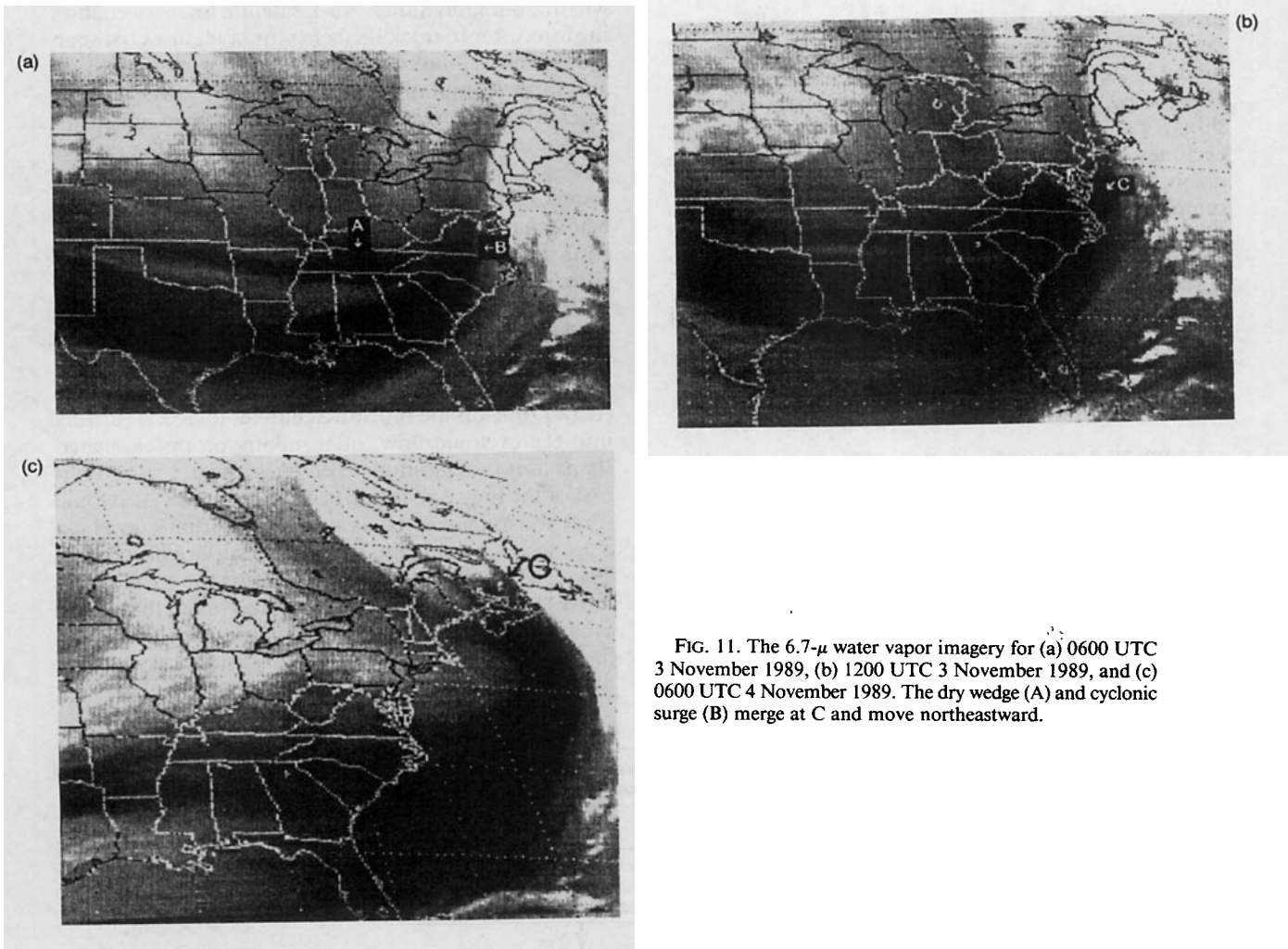

FIG. 11. The 6.7-μ water vapor imagery for (a) 0600 UTC 3 November 1989, (b) 1200 UTC 3 November 1989, and (c) 0600 UTC 4 November 1989. The dry wedge (A) and cyclonic surge (B) merge at C and move northeastward.

(b) Smigielski and Ellrod (1985) point out that when an elliptical dark band develops behind an S-shaped pattern in the water vapor imagery, the associated cloud system will move rapidly, and the system will usually deepen until the dark band becomes diffuse. The dark band will become elongated and larger as cyclogenesis progresses.

(c) According to Beckman (1987), a well-defined "hook" pattern in the water vapor imagery often indicates a strong vorticity center. The hook feature is caused by partial dry slot entrainment near the vorticity center, which helps to define the classic PVA comma cloud. This feature can be particularly useful when evaluating dynamical model output.

(d) Weldon (1985) and Gurka (1987) have shown that there are often dark bands on moisture channel imagery associated with 500-mb troughs, with the most distinct patterns at the base of digging troughs. This is a good example of an upper-level trigger mechanism that can be tracked on the moisture channel data. Observations of rapidly deepening storms from 1988 through 1990 indicate that the leading edge of a dark band within a 500-mb trough is often associated with a 500-mb speed maxima.

(e) As previously discussed, the jet stream plays a critical role in explosive cyclogenesis. Weldon (1985) showed that water vapor patterns can often be used to locate jet axes. Weldon and Holmes (1991) present detailed descriptions of the water vapor imagery patterns associated with different jet structures.

To further identify water vapor features associated with rapidly deepening storms, moisture channel imagery from 16 cases of explosive East Coast cyclogenesis, between 35° and 50°N lat and from 75°W E to 55°W long, during the 1988–89 and 1989–90 cool seasons (October through March), were analyzed. This is a subset of the 29 bombs observed during this period and used for the bomb checklist verification discussed in section 3b. One particular feature that was prominent in all of the cases was a rapid propagation of dry air at middle and upper levels moving toward the cyclogenetic region during and preceding rapid deepening. For the remainder of this section, this feature will be referred to as a dry surge. These dry surges appeared

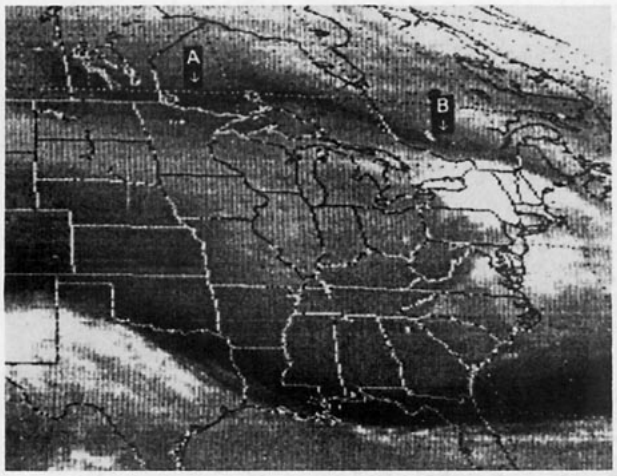

FIG. 12. The 6.7-μ water vapor image for 1100 UTC 20 November 1989. Dry wedges are evident at A and B.

as dark wedges, or bands, on moisture channel imagery with a conventional enhancement curve (i.e., white = cold, and black = warm).

Often, the leading edge of the dry surges were associated with a 500-mb wind speed maximum. During and just prior to rapid deepening, the dry surges tended to move rapidly, increase in area, and become warmer (drier) and better defined. Perhaps one mechanism for this rapid warming apparent on the moisture channel imagery could be tropopause folding, and an associated extrusion of stratospheric air into the troposphere as defined by Reed (1955) and Reed and Danielsen (1959). Uccellini et al. (1985), Uccellini (1986), and Whitaker et al. (1988) used case studies to illustrate the processes that link jet structures and associated tropopause folds with subsequent rapid surface cyclogenesis. For a more complete discussion on stratospheric extrusions, tropopause folds, and the contribution of potential vorticity to surface cyclogenesis, the reader is referred to Uccellini (1990) and Reed et al. (1992).

In examining satellite data for features associated with cyclogenesis, the value of time-lapse imagery cannot be over emphasized. Before rapid deepening is imminent, the dry surge associated with a short-wave trough can sometimes be very subtle, and difficult to identify on a single image.

There were two types of dry surges associated with the rapidly deepening storms: 1) a narrow, wedge-shaped band (dry wedge), typically associated with an upper short-wave trough, moving from the west or northwest; and 2) a more widespread dry band that surged toward the north or northeast along the baroclinic zone, subsequently becoming the dry slot. As discussed previously, Weldon (1985) refers to this feature as "cyclonic surge warming." Generally, cyclonic surges were wider, more extensive, and drier (warmer or darker) than the dry wedges.

Typically, when a dry wedge (e.g., short-wave trough) approaches the cyclogenetic region, the cyclonic surge along the baroclinic zone will become more pronounced, often merging with the dry wedge into a single expanded dry area. For 8 of the 16 cases, the dry wedge merged with the cyclonic surge, generally resulting in an acceleration of the surge along the baroclinic zone. This type of evolution is consistent with Evans et al. (1994) "left exit" and "instant occlusion" conceptual models.

An example of a dry wedge–cyclonic surge merger occurred on 3–4 November 1989. Figure 11a, at 0600 UTC 3 November 1989, depicts a distinct dry wedge (A) over Tennessee, and the leading edge of a cyclonic surge (B) over southern Virginia. By 1200 UTC (Fig. 11b), the dry wedge and the cyclonic surge were beginning to merge over the Delmarva Peninsula (C). At this time, a 1008-mb surface low was developing along the mid-Atlantic coast. During the subsequent 18–24 h, the dry wedge and cyclonic surge merged and tracked rapidly northeastward, reaching the Canadian Maritimes at 0600 UTC 4 November 1989 (Fig. 11c). By 1200 UTC, the associated surface low deepened to 988 mb.

For three of the 16 cases, the dry wedge associated with the short-wave trough evolved into a cyclonic surge as development occurred within the cold air. This is similar to the "emerging cloud head" model suggested by Evans et al. (1994). November 20–21 1989 was an example of rapid cyclogenesis in which a dry wedge associated with a vigorous 500-mb short-wave trough moved rapidly southeast across the Great Lakes. This dry wedge subsequently evolved into a cyclonic surge as it approached the East Coast, resulting in deepening of the surface cyclone.

The leading edge of the dry wedge at 1100 UTC 20 November 1989, is indicated at "A" on Fig. 12. Figure 13 reveals that this dry wedge was associated with a wind maximum at the base of a 500-mb trough, as indicated by the 59 and 51 m s^{-1} (115 and 100 kt) wind speeds at International Falls, Minnesota (INL), and St. Cloud, Minnesota (STC), respectively. At 1200 UTC 20 November 1989, a 989-mb surface low was located north of Sault St. Marie, Michigan (not shown). Note, a second, somewhat less distinct dry wedge (indicated by "B" in Fig. 12) was collocated with a 51 m s^{-1} (100 kt) relative speed maxima located over Maniwaki, Quebec.

The dry wedge A was quite apparent in subsequent imagery as it first tracked southeastward to the East Coast (Figs. 14a–c), and subsequently evolved into a cyclonic surge when it accelerated to the northeast along the baroclinic zone (Figs. 14d–e). Dry wedge B became considerably less distinct after 1400 UTC (Fig. 14a). A comma head pattern began to evolve by 0000 UTC ("C" on Fig. 14b). Note, most of dry surge A was initially along or upstream of the 500-mb trough (Figs. 12 and 13). However, as development progressed, the leading edge of dry wedge A accelerated as it evolved into a cyclonic surge, eventually moving downstream of the trough axis. This is evident

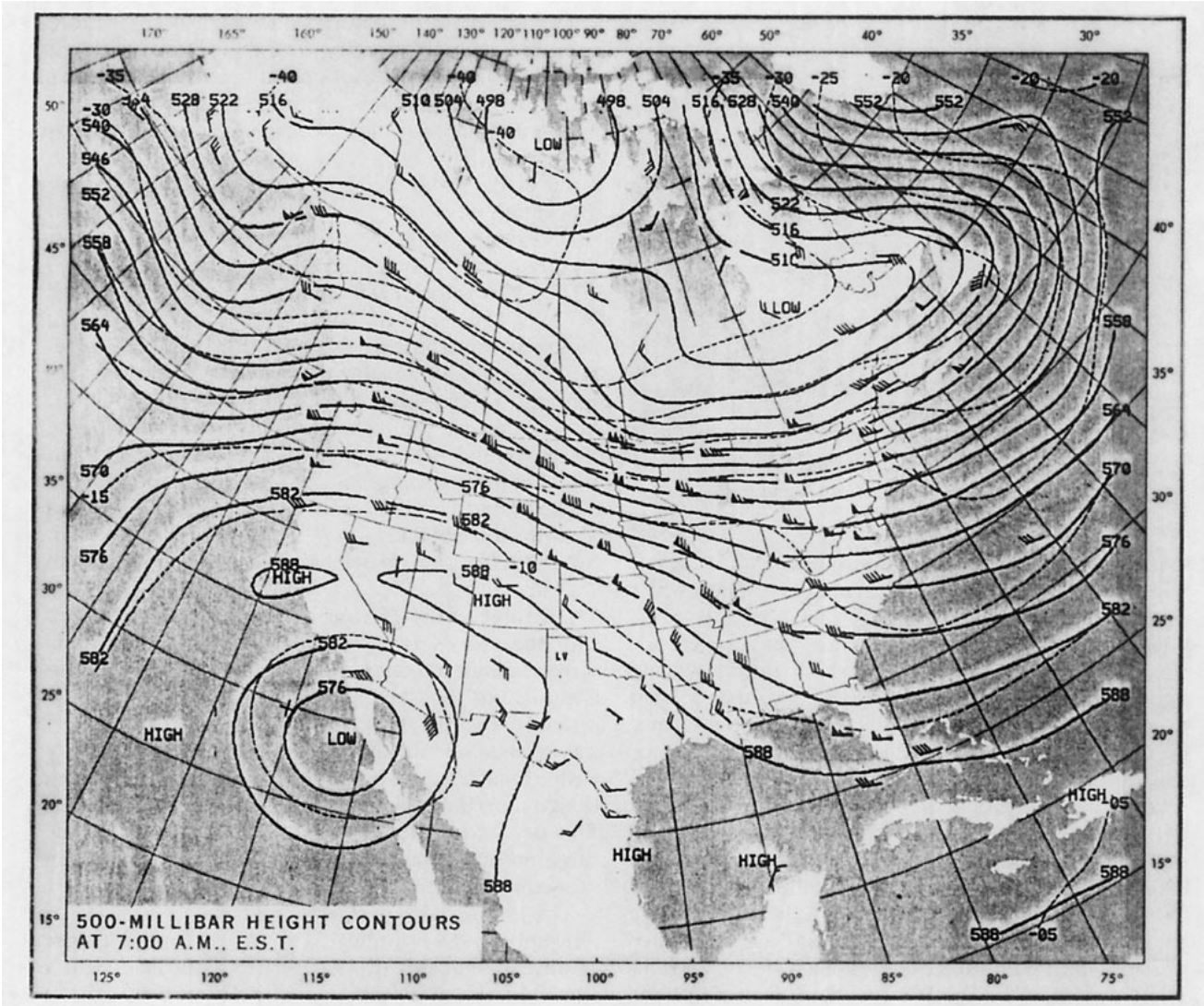

FIG. 13. The 500-mb analysis for 1200 UTC 20 November 1989.

in Fig. 14e, and Fig. 15, the 500-mb analysis for 1200 UTC 21 November 1989. By this time, the surface low had redeveloped along the New England coast and deepened to 968 mb over the Gulf of Maine. The storm continued to develop rapidly as it tracked northeast, deepening to 963 mb at 1800 UTC 21 November 1989.

Rapid deepening of the surface low occurred from 1800 UTC 20 November to 1800 UTC 21 November 1989. During this time, the dry surge moved rapidly, and became more distinct and extensive. The mean speed of the leading edge of dry surge A, from the time rapid deepening began (1800 UTC 20 November 1989) until the time when the dry surge began to wrap around the upper low center (1200 UTC 21 November 1989; Fig. 14e), was approximately 27 m s^{-1} (53 kt). The maximum speed for at least a 2-h period during rapid deepening was 29 m s^{-1} (56 kt). The maximum speed during the 6 h immediately preceding explosive deepening was 58 m s^{-1} (114 kt) between 1200 and 1500 UTC on 20 November 1989. This speed refers to the displacement of the leading edge of the dry surge. Since the displacement incorporates both motion and growth, propagation might be a more accurate term, but speed is used here for the sake of simplicity.

Dry surge speeds were computed for all of the 16 explosive cyclogenesis cases, from t_0 (the start of rapid deepening) until the dry surge began to wrap around the upper low (usually indicative of a cyclone entering the filling stage). The average speed during the period of rapid deepening for the 16 cases studied was 27 m s^{-1} (53 kt). Average speeds for 12 of the 16 cases were between 22 and 29 m s^{-1} (43–57 kt), while the other four cases had average speeds between 32 and 42 m s^{-1} (62–82 kt). For most of the cases, speeds were averaged over at least a 15-h period.

The maximum speeds averaged over at least a 2-h period during rapid deepening ranged from 26 to 51

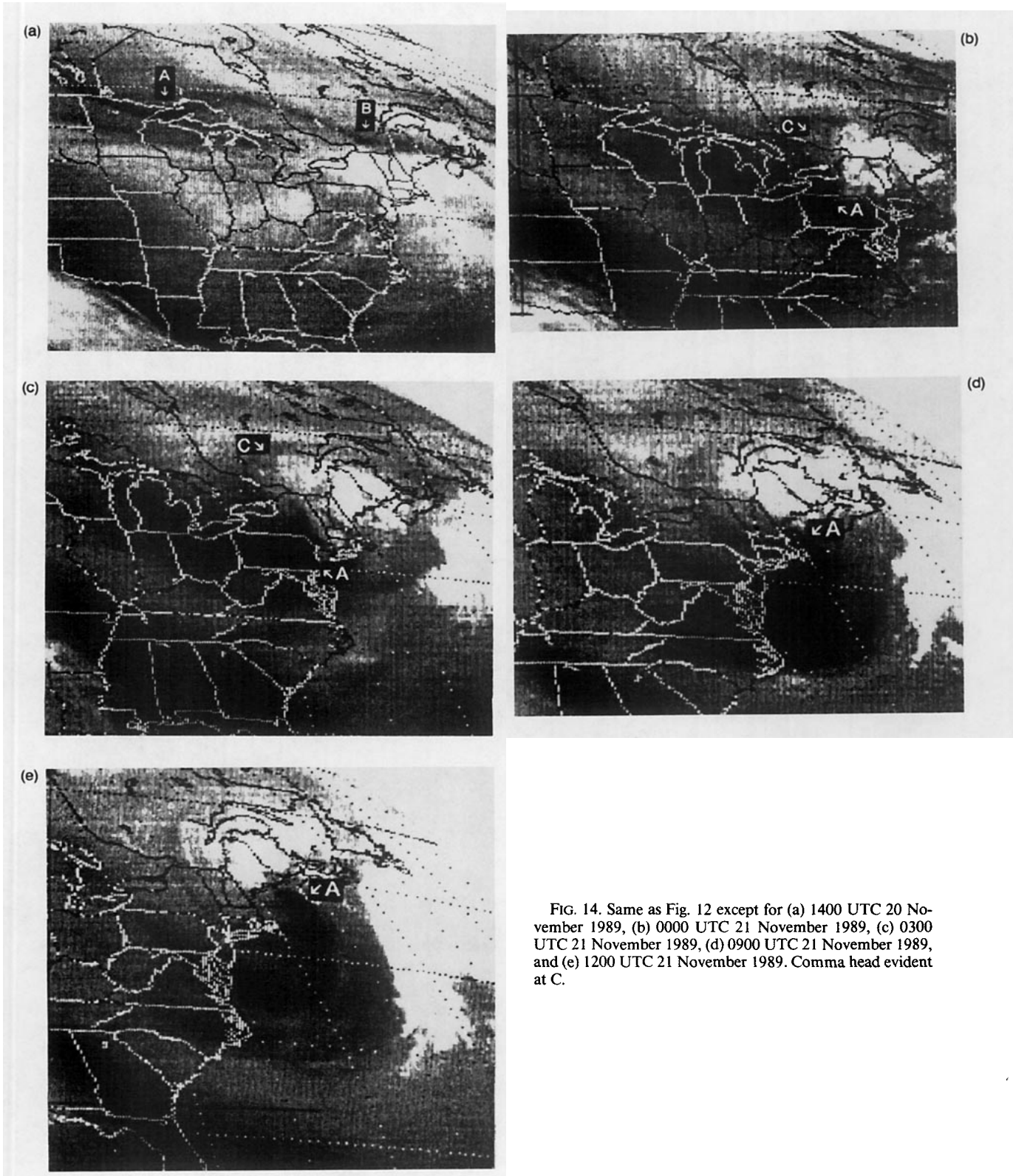

FIG. 14. Same as Fig. 12 except for (a) 1400 UTC 20 November 1989, (b) 0000 UTC 21 November 1989, (c) 0300 UTC 21 November 1989, (d) 0900 UTC 21 November 1989, and (e) 1200 UTC 21 November 1989. Comma head evident at C.

m s^{-1} (51–99 kt), with an average maximum speed of 38 m s^{-1} (74 kt). During the first 6 h of rapid deepening, all of the 16 cases showed dry surge speeds of 25 m s^{-1} (48 kt) or greater for at least a 2-h period. For the 6-h period prior to rapid deepening (T_{0-6}), moisture channel imagery was available for only 12 of the 16 cases. Ten of these 12 cases had dry surge speeds of 25 m s^{-1} (48 kt) or greater for at least a 2-h period.

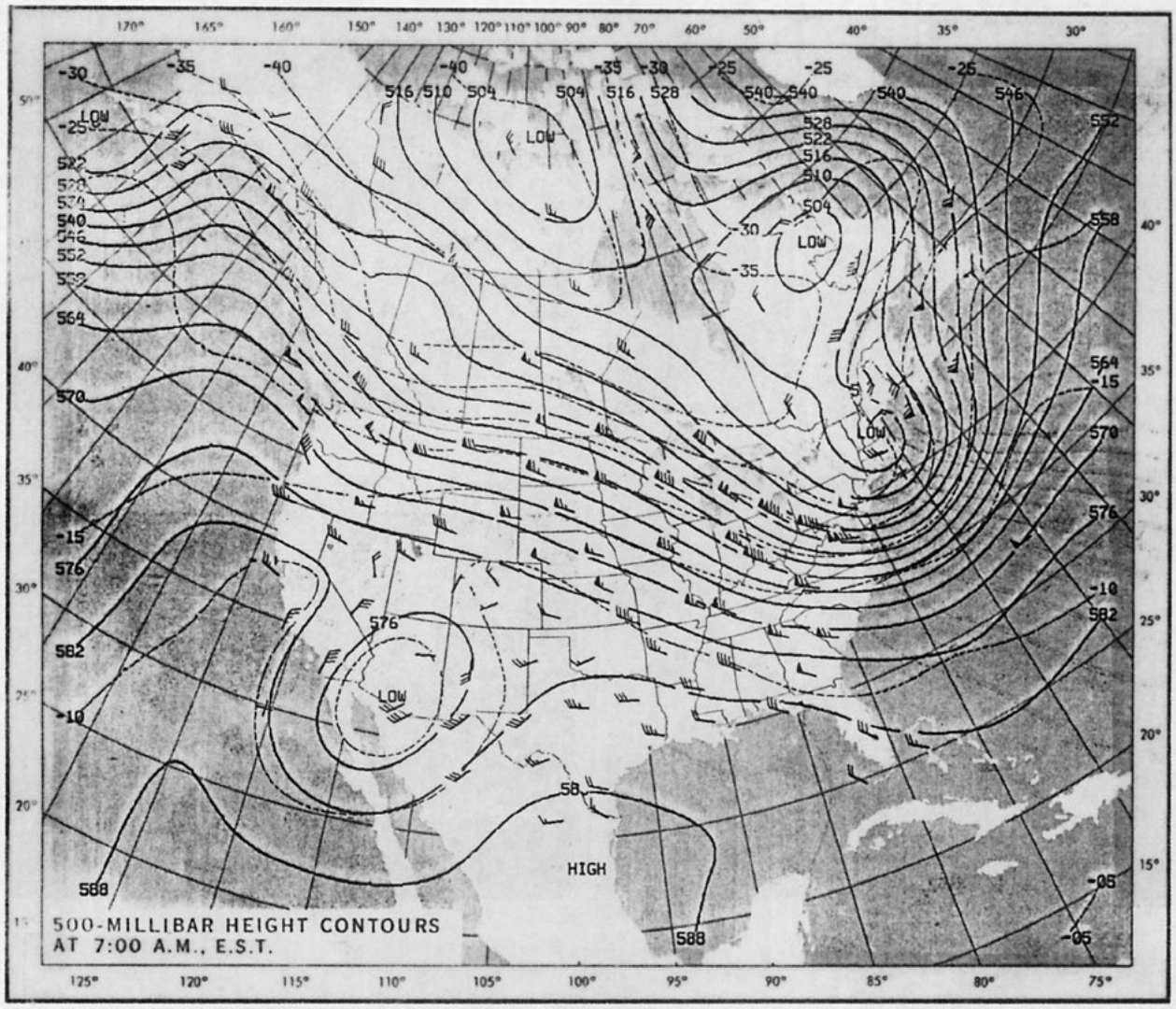

FIG. 15. The 500-mb analysis for 1200 UTC 21 November 1989.

Six of the cases had dry surge speeds of 40 m s^{-1} (78 kt) or greater, while three had dry surge speeds in excess of 52 m s^{-1} (100 kt). Based on these values, it appears that an acceleration of a dry surge (toward a baroclinic zone) with speeds in excess of 25 m s^{-1} may be an indication of the initiation of rapid cyclogenesis, particularly if the increased dry surge speed persists.

It should be noted that satellite imagery in analog form was used in this study. Hence, some of these insights, such as expansion of the dry surges and changes in the sharpness or definition of the dry surges, were based on subjective visual impressions. However, many of these observations are consistent with the findings of Weldon (1985) and Smigielski and Ellrod (1985). Further study with digital data on interactive workstations is necessary to quantitatively relate the rate of drying (warming) and changes in the size of dry areas, with the rate of deepening. In addition, a thorough examination of features associated with lows that did not deepen rapidly has not been conducted. Future research might focus on comparing factors such as the rate of expansion; speed of the leading edge; the rate of warming; and the definition of dry surges (diffuse vs well defined) for storms that deepened rapidly and those that did not.

Finally, for the operational use of moisture channel imagery, time-lapse loops, and an enhancement curve with sufficient contrast, can be of great assistance in analyzing the sometimes subtle features associated with upper-level troughs preceding the onset of rapid deepening. Also, since dark bands similar to the ones described here can be associated with other features, such as deformation zones, it is essential that forecasters use *all* available data (e.g., upper-air observations, dynamical model output, etc.), in conjunction with the imagery to help determine those features that are associated with potential upper-level triggers. Moisture channel data can then be a valuable tool in tracking

the upper-level troughs and/or speed maxima that can initiate explosive development. Provided the necessary ingredients for rapid deepening are available, when a dry wedge associated with an upper trough or speed maximum rapidly approaches a baroclinic zone along the East Coast, the water vapor imagery should be carefully monitored for development or rapid growth of a cyclonic surge.

5. Summary and concluding remarks

This document has presented cyclogenesis from the perspective of an operational forecast problem. Different patterns of cyclogenesis were discussed, and some of the dynamical model and satellite-derived techniques for diagnosing and forecasting cyclogenesis have been presented. It may appear from the previous discussions that much of the current methodology for diagnosing cyclogenetic potential employed in the operational environment is rooted in paradigmatic recognition. Perhaps this is an adequate reflection of the state of the art that has historically existed in the operational community. During the past decade, field projects, such as the Genesis of Atlantic Lows Experiment (GALE; Dirks 1988) and ERICA, in combination with model diagnostic studies (Whitaker et al. 1988; Reed et al. 1992, among numerous others), have brought a wealth of knowledge and insight into the processes associated with cyclogenesis, and the development of advanced conceptual models. However, these discoveries relied on the use of high-resolution surface and upper-air observations, information from new remote sensing technologies such as Doppler radar, high-resolution gridded output from dynamical models, and the computational power necessary to integrate and manipulate these data.

It is only very recently that operational forecasters have gained access to these resources. The value of forecaster access to gridded model data has been demonstrated by Dunn (1991), Baker (1991), Weismueller and Brady (1993), Niziol and Mclaughlin (1992), Zubrick and Thaler (1993), and Gates and Zubrick (1993), among others. As discussed in the companion paper by Maglaras et al. (1995), the deployment of new high-resolution remote sensors—such as the Weather Surveillance Radar 1988, Doppler (WSR-88D), and the Automated Surface Observing System (ASOS) networks (U.S. Department of Commerce 1994b)—and the development of operational mesoscale dynamical models (Baker et al. 1992; Black 1994) will go a long way to assist with the development of new operational techniques and applications that will more fully utilize the recent advances in cyclogenetic theory.

Finally, an aggressive integrated training and professional development plan (U.S. Department of Commerce 1992b) has been formulated to take advantage of these new technological innovations and the accompanying advances in the theory. At the heart of this plan is the Cooperative Program for Operational Meteorology, Education, and Training (COMET). COMET is a joint effort among the operational, academic, and research communities. This provides a unique opportunity for operational meteorologists to gain the benefits of recent scientific advances and research efforts, while academic and research participants learn more about the operational aspects of the science. It is anticipated that this new approach will substantially narrow the gap, and result in a greater blending of conceptual meteorology and operational applications.

Acknowledgments. The authors are indebted to Dick Pritchard of the Satellite Applications Laboratory, NESDIS, for providing the hardcopy satellite imagery, and to the WSFO Albany Mesoscale Climatology Project for providing selected surface and upper-air data. Special thanks also to Paul Kocin of NMC for drafting Fig. 1. We would also like to thank Gary Carter and Paul Stokols of the Scientific Services Division, National Weather Service Eastern Region Headquarters, and three anonymous reviewers for their insightful comments and suggestions for improving this manuscript.

REFERENCES

Anderson, R. K., 1987: Diagnosing explosive cyclogenesis in the west central North Atlantic Ocean using animated satellite imagery. *Proc. Second Workshop on Operational Meteorology,* Halifax, Canada, Canadian Meteorology and Oceanography Society, 4 pp.

——, 1989: The use of satellite data for the analysis of oceanic storms during the Experiment on Rapidly Intensifying Cyclones over the Atlantic (ERICA). Preprints, *12th Conf. on Weather Analysis and Forecasting,* Monterey, CA, Amer. Meteor. Soc., 511–514.

Auciello, E. P., 1989: A method for predicting meteorological bombs in the western North Atlantic Ocean. Postprints, *Second National Winter Weather Workshop,* Raleigh, NC, NOAA/NWS, 209–217.

——, and F. Sanders, 1986: An operational checklist for the forecasting of explosive cyclogenesis in the North Atlantic Ocean. Eastern Region Technical Attachment No. 86-7, 5 pp. [Available from the Scientific Services Division, NWS Eastern Region Headquarters, Bohemia, NY 11716.]

——, and ——, 1987: An operational checklist for the forecasting of explosive cyclogenesis in the North Atlantic Ocean. *Proc. Second Workshop on Operational Meteorology,* Halifax, Canada, Canadian Meteor. and Ocean. Society, 49–55.

——, and ——, 1988: Bomb checklist and the 1987–88 cold season. Eastern Region Technical Attachment No. 88-17(B), 3 pp. [Available from the Scientific Services Division, NWS Eastern Region Headquarters, Bohemia, NY 11716.]

Austin, J. M., 1941: Favorable conditions for cyclogenesis near the Atlantic coast. *Bull. Amer. Meteor. Soc.,* **22,** 270–272.

Baker, D. V., 1991: Experimental use of gridded NGM output at WSFO Lubbock, Texas: An initial report. NOAA Tech. Memo. NWS SR-139, NOAA/NWS, Fort Worth, TX, 19 pp.

Baker, W. E., E. Kalnay, M. Kanamitsu, and R. Petersen, 1992: NMC analysis and modeling plans in support of the NWS modernization. *Symp. on Weather Forecasting,* Atlanta, GA, Amer. Meteor. Soc., 9 pp. [Available from National Meteorological Center, Development Division, Washington, DC 20233.]

Beckman, S. K., 1987: Operational use of water vapor imagery. NOAA Tech. Memo. NWS CR-87, NOAA/NWS, Kansas City, MO, 15 pp.

Black, T. L., 1994: The new NMC mesoscale eta model: Description and forecast examples. *Wea. Forecasting,* **9,** 265–278.

Bosart, L. F., 1981: The Presidents' Day snowstorm of 18–19 February 1979: A subsynoptic-scale event. *Mon. Wea. Rev.,* **109,** 1542–1566.

——, and F. Sanders, 1991: An early-season coastal storm: Conceptual success and model failure. *Mon. Wea. Rev.,* **119,** 2831–2851.

Browning, K. A., 1990: Organization of clouds and precipitation in extratropical cyclones. *Extratropical Cyclones: The Erik Palmén Memorial Volume,* C. W. Newton and E. O. Holopainen, Eds., Amer. Meteor. Soc., 129–153.

——, and F. F. Hill, 1985: Mesoscale analysis of a polar trough interacting with a polar front. *Quart. J. Roy. Meteor. Soc.,* **111,** 445–462.

Businger, S., and R. J. Reed, 1989: Polar lows. *Polar and Arctic Lows,* P. F. Twitchell, E. A. Rasmussen, and K. L. Davidson, Eds., A. Deepack, 3–45.

Clark, D. A., 1983: A comparative study of coastal frontogenesis. M.S. thesis, Massachusetts Institute of Technology, Cambridge, MA, 86 pp.

Davis, R. E., R. Dolan, and G. Demme, 1993: Synoptic climatology of Atlantic coast north-easters. *Int. J. Climatol.,* **13,** 171–189.

Dirks, R. A., J. P. Kuettner, and J. A. Moore, 1988: Genesis of Atlantic Lows Experiment (GALE)—An overview. *Bull. Amer. Meteor. Soc.,* **69,** 148–160.

Dunn, L. B., 1991: Evaluation of vertical motion, past, present, and future. *Wea. Forecasting,* **6,** 65–75.

Dvorak, V. F., 1984: Tropical cyclone analysis using satellite data. NOAA Tech. Rep. NESDIS 11, NOAA/NESDIS, Washington, DC, 47 pp.

Evans, M. S., D. Keyser, L. F. Bosart, and G. L. Lackmann, 1994: A satellite-derived classification scheme for rapid maritime cyclogenesis. *Mon. Wea. Rev.,* **122,** 1381–1416.

Fishel, G. B., and S. Businger, 1993: Heavy orographic snowfall in the southern Appalachians: A late season case study. Postprints, *Third National Heavy Precipitation Workshop,* Pittsburgh, PA, NOAA/NWS, 275–284.

Fritsch, J. M., J. Kapolka, and P. A. Hirschberg, 1992: The effects of subcloud-layer diabatic processes on cold air damming. *J. Atmos. Sci.,* **49,** 49–70.

Funk, T. W., 1986: The use of water vapor imagery in the analysis of the November 1985 Middle Atlantic states record flood event. *Natl. Wea. Dig.,* **11,** 12–19.

Gates, C., and S. Zubrick, 1993: PC-GRIDDS as a supplement to standard NGM guidance. Preprints, *13th Conf. on Weather Analysis and Forecasting,* Vienna, VA, Amer. Meteor. Soc., 79–85.

Gigi, A. F., 1989: The New York City snowstorm that never was. Eastern Region Technical Attachment 89-14, 12 pp. [Available from the Scientific Services Division, NWS Eastern Region Headquarters, Bohemia, NY 11716.]

Grumm, R. H., 1993: Characteristics of surface cyclone forecasts in the aviation run of the global spectral model. *Wea. Forecasting,* **8,** 87–112.

——, and A. L. Siebers, 1989: Systematic surface cyclone errors in NMC's Nested Grid Model, November 1988–January 1989. *Wea. Forecasting,* **4,** 246–252.

——, and ——, 1990: Systematic model forecast errors of surface cyclones in the NGM and AVN, January 1990. *Wea. Forecasting,* **5,** 672–682.

——, R. J. Oravec, and A. L. Siebers, 1992: Systematic model forecast errors of surface cyclones in NMC's Nested Grid Model, December 1988 through November 1990. *Wea. Forecasting,* **7,** 65–87.

Gurka, J. J., 1987: Examples showing how analysis of water vapor imagery suggests modification to numerical model analysis and prediction. Preprints, *Workshop on Satellite and Radar Imagery Interpretation,* Reading, England, EUMETSAT, 125–141.

Gyakum, J. R., 1983: One the evolution of the QE II Storm II: Dynamic and thermodynamic structure. *Mon. Wea. Rev.,* **111,** 1156–1173.

Hadlock, R., and C. W. Kreitzberg, 1988: The Experiment on Rapidly Intensifying Cyclones over the Atlantic (ERICA) field study—Objectives and plans. *Bull. Amer. Meteor. Soc.,* **69,** 1309–1320.

Hoke, J. E., N. A. Phillips, G. J. DiMego, J. J. Tuccillo, and J. G. Sela, 1989: The regional analysis and forecast system of the National Meteorological Center. *Wea. Forecasting,* **4,** 323–334.

Junker, N. W., and D. J. Haller, 1980: Estimation of surface pressure by satellite cloud pattern recognition, Preprints, *Eighth Conf. on Weather Forecasting and Analysis,* Denver, CO, Amer. Meteor. Soc., 119–122.

——, J. E. Hoke, and R. H. Grumm, 1989: Performance of NMC's regional models. *Wea. Forecasting,* **4,** 368–390.

Kanamitsu, M., 1989: Description of the NMC Global Data Assimilation and Forecast System. *Wea. Forecasting,* **4,** 335–342.

Keeter, K. K., J. W. Cline, and R. P. Green, 1989: Local objective guidance for predicting precipitation type (LOG/PT) in North Carolina—An alternative to MOS guidance. Postprints, *Second National Winter Weather Workshop,* Raleigh, NC, NOAA/NWS, 125–135.

——, S. Businger, and L. G. Lee, 1993: Patterns of winter precipitation types across North Carolina. Preprints, *13th Conf. on Weather Analysis and Forecasting,* Vienna, VA, Amer. Meteor. Soc., 528–532.

——, S. Businger, L. G. Lee, and J. S. Waldstreicher, 1995: Forecasting winter weather throughout the eastern United States. Part III: The effects of topography and the variability of winter weather in the Southeast. *Wea. Forecasting,* **10,** 42–60.

Keshishian, L. G., and L. F. Bosart, 1987: A case of extended east coast frontogenesis. *Mon. Wea. Rev.,* **115,** 100–117.

Kocin, P. J., and L. W. Uccellini, 1990: *Snowstorms along the Northeastern Coast of the United States: 1955–1985. Meteor. Monogr.,* No. 44, Amer. Meteor. Soc., 280 pp.

Lange, O., R. Fett, R. Landis, G. Wells, G. Rasch, E. Auciello, M. Horita, and J. Jannuzzi, 1986: Summary of a workshop/seminar on oceanic storms 9–13 September 1985, Seattle, Washington. *Bull. Amer. Meteor. Soc.,* **67,** 1272–1277.

Leary, C., 1971: Systematic errors in operational National Meteorological Center primitive equation surface prognoses. *Mon. Wea. Rev.,* **99,** 409–413.

Maglaras, G. J., J. S. Waldstreicher, P. J. Kocin, A. F. Gigi, and R. A. Marine, 1995: Winter weather forecasting throughout the eastern United States. Part I: An overview. *Wea. Forecasting,* **10,** 5–20.

Mather, J. R., H. Adams, and G. A. Yoshikoa, 1964: Coastal storms of the eastern United States. *J. Appl. Meteor.,* **3,** 693–706.

Miller, J. E., 1946: Cyclogenesis in the Atlantic coastal region of the United States. *J. Meteor.,* **3,** 31–44.

National Weather Service, 1994: Disaster survey report: The great nor'easter of December 1992. NOAA/NWS, Bohemia, NY, 67 pp.

Niziol, T. A., and S. Mclaughlin, 1992: The use of high resolution data from the Nested Grid Model for the prediction of lake effect snows. Postprints, *Third Natl. Winter Weather Workshop,* Portland, OR, NOAA/NWS, 11 pp.

Oravec, R. J., and R. H. Grumm, 1993: The prediction of rapidly deepening cyclones by NMC's Nested Grid Model: Winter 1989 through Autumn 1991. *Wea. Forecasting,* **8,** 248–270.

Pettersen, S., and S. J. Smebye, 1971: On the development of extratropical storms. *Quart. J. Roy. Meteor. Soc.,* **97,** 457–482.

Reed, R. J., 1955: A study of a characteristic type of upper-level frontogenesis. *J. Meteor.,* **12,** 226–237.

——, and E. F. Danielsen, 1959: Fronts in the vicinity of the tropopause. *Arch. Meteor. Geofys. Bioklimatol.,* **A11,** 1–17.

——, M. T. Stoelinga, and Y.-H. Kuo, 1992: A model-aided study of the origin and evolution of the anomalously high potential vorticity in the inner region of a rapidly deepening marine cyclone. *Mon. Wea. Rev.,* **120,** 893–913.

Richwein, B. A., 1980: The damming effect of the southern Appalachians. *Natl. Wea. Dig.,* **5,** 2–12.

Roebber, P. J., 1984: Statistical analysis and updated climatology of explosive cyclones. *Mon. Wea. Rev.,* **112,** 1577–1589.

Sabones, M. E., and K. K. Keeter, 1989: Late season snowfalls in the North Carolina mountains associated with cut-off lows. Postprints, *Second National Winter Weather Workshop,* Raleigh, NC, 230–236.

Sanders, F., 1986: Explosive cyclogenesis over the west central North Atlantic Ocean, 1981–1984. Part I: Composite structure and mean behavior. *Mon. Wea. Rev.,* **114,** 1781–1794.

——, 1987a: A study of 500 mb vorticity maxima crossing the east coast of North America and associated surface cyclogenesis. *Wea. Forecasting,* **2,** 70–83.

——, 1987b: Skill of NMC operational dynamical model in prediction of explosive cyclogenesis. *Wea. Forecasting,* **2,** 322–336.

——, 1992: Skill of operational dynamical models in cyclone prediction out to five-days range during ERICA. *Wea. Forecasting,* **7,** 3–25.

——, and J. R. Gyakum, 1980: Synoptic–dynamic climatology of the "bomb." *Mon. Wea. Rev.,* **108,** 1590–1606.

——, and E. P. Auciello, 1989: Skill in prediction of explosive cyclogenesis over the western North Atlantic Ocean, 1987/88: A forecast checklist and NMC dynamical models. *Wea. Forecasting,* **4,** 157–172.

Scofield, R. A., 1990: Instability bursts associated with extratropical cyclone systems (ECSs) and a forecast index of 3–12 h heavy precipitation. NOAA Tech. Memo. NESDIS 30, NOAA/NESDIS, Washington, DC, 77 pp.

Sela, J. G., 1980: Spectral modeling at NMC. *Mon. Wea. Rev.,* **108,** 1279–1292.

Silberberg, S. R., and L. F. Bosart, 1982: An analysis of systematic cyclone errors in the NMC LFM-II model during the 1978–1979 cool season. *Mon. Wea. Rev.,* **110,** 254–271.

Smigielski, F. J., and G. P. Ellrod, 1985: Surface cyclogenesis as indicated by satellite imagery. NOAA Tech. Memo. NESDIS 9, NOAA/NESDIS, Washington, DC, 30 pp.

——, and H. M. Mogil, 1991: Use of satellite information for improved oceanic surface analysis. Preprints, *First Int. Symp. an Winter Storms,* New Orleans, LA, Amer. Meteor. Soc., 137–144.

——, and ——, 1992: A systematic satellite approach for estimating central surface pressures of mid-latitude oceanic storms. NOAA Tech. Rep. NESDIS 63, NOAA/NESDIS, Washington, DC, 64 pp.

Smith, B. B., and S. L. Mullen, 1993: An evaluation of sea level cyclone forecasts produced by NMC's Nested Grid Model and Global Spectral Model. *Wea. Forecasting,* **8,** 37–56.

Tracton, M. S., 1973: The role of cumulus convection in the development of extratropical cyclones. *Mon. Wea. Rev.,* **101,** 573–592.

——, and E. Kalnay, 1993: Operational ensemble prediction at the National Meteorological Center: Practical aspects. *Wea. Forecasting,* **8,** 379–398.

Uccellini, L. W., 1986: The possible influence of upstream upper-level baroclinic processes on the development of the QE II storm. *Mon. Wea. Rev.,* **114,** 1019–1027.

——, 1990: Processes contributing to the rapid development of extratropical cyclones. *Extratropical Cyclones: The Erik Palmén Memorial Volume,* C. W. Newton and E. O. Holopainen, Eds., Amer. Meteor. Soc., 81–105.

——, D. Keyser, K. F. Brill, and C. H. Wash, 1985: The Presidents' Day cyclone of 18–19 February 1979: Influence of upstream trough amplification and associated tropopause folding on rapid cyclogenesis. *Mon. Wea. Rev.,* **113,** 962–988.

U.S. Department of Commerce, 1992a: *Storm Data,* **34** (5).

——, 1992b: Integrated training and professional development plan for the modernization and associated restructuring of the National Weather Service. NOAA/NWS, Office of Meteorology, Washington DC, 230 pp.

——, 1994a: Natural disaster survey report: Superstorm of March 1993. NOAA/NWS, Silver Spring, MD, 152 pp.

——, 1994b: National implementation plan for the modernization of the National Weather Service for fiscal year 1995. NOAA, Washington DC, 208 pp.

Weldon, R. B., 1975: The structure and evolution of winter storms. Satellite training course notes, Part II. [Available from the Satellite Applications Laboratory, NOAA/NESDIS, World Weather Building, Washington, DC 20233.]

——, 1979: Upper wind field. Satellite training course notes, Part IV. AWS/TR-79/003, 80 pp. [Available from the Satellite Applications Laboratory, NOAA/NESDIS, World Weather Building, Washington, DC 20233.]

——, 1985: Conclusions and generalizations: Water vapor image gray shades vs. moisture distribution. 6 pp. [Available from the Satellite Applications Laboratory, NOAA/NESDIS, World Weather Building, Washington, DC 20233.]

——, and S. J. Holmes, 1991: Water vapor imagery: Interpretation and applications to weather analysis and forecasting. NOAA Tech. Rep. NESDIS 57, NOAA/NESDIS, Washington, DC, 213 pp.

Whitaker, J. S., L. W. Uccellini, and K. F. Brill, 1988: A model-based diagnostic study of the rapid development phase of the Presidents' Day cyclone. *Mon. Wea. Rev.,* **116,** 2337–2365.

Wiesmueller, J. L., and R. H. Brady, 1993: A Mid-Atlantic rain event: A review and comparison of techniques for assessing vertical motion. *Natl. Wea. Dig.,* **18,** 31–54.

Young, M. V., 1993: Cyclogenesis: Interpretation of satellite and radar images for the forecaster. Forecasting Research Division Tech Rep. No. 73, United Kingdom Meteorological Office. [Available from Forecasting Research Division, Meteorological Office, London Rd., Bracknell, Berkshire Rg12 2SZ, United Kingdom.]

Zubrick, S. M., and E. Thaler, 1993: Enhancements to the operational forecast process using gridded model data. Preprints, *13th Conf. on Weather Analysis and Forecasting,* Vienna, VA, Amer. Meteor. Soc., 5–9.